Synthesis and Application of Indole and Carbazole Based Organic Dyes in Dye Sensitized Solar Cells

A project report submitted

as a part of requirements for the degree of

MASTER OF SCIENCE

By

KUNTAL PAL

Roll no. CY13M1009

Under the supervision of

Dr. D. S. Sharada

DEPARTMENT OF CHEMISTRY

INDIAN INSTITUTE OF TECHNOLOGY HYDERABAD

INDIA

APRIL 2015

Declaration

I declare that this written submission represents my ideas in my own words, and where others' ideas or words have been included, I have adequately cited and referenced the original sources. I also declare that I have adhered to all principles of academic honesty and integrity and have not misrepresented or fabricated or falsified any idea/data/fact/source in my submission. I understand that any violation of the above will be a cause for disciplinary action by the Institute and can also evoke penal action from the sources that have thus not been properly cited, or from whom proper permission has not been taken when needed.

Kuntal Pal.

(Student signature)

KUNTAL PAL

(Student Name)

CY13M1009

(Roll No)

Approval Sheet

This thesis entitled **"Synthesis and application of Indole and Carbazole based organic dyes in dye sensitized solar cells"** by *Kuntal Pal* is approved for the degree of Master of Science from IIT Hyderabad.

Dr. SURENDRA K. MARTHA
Assistant Professor
Department of Chemistry
Indian Institute of Technology Hyderabad

-Name and affiliation-
Examiner

Dr. SU ARTHA
Assi... Prof.
Department of Chemistry
Indian Institute of Technology Hyderabad

-Name and affiliation-
Examiner

Dr. G. Satyanarayana
Associate Professor
Department of Chemistry
Indian Institute of Technology Hyderabad
Ordnance Factory Estate, Yeddumailar

-Name and affiliation-
Adviser

Dr. D. S. SHARADA
Assistant Professor
Department of Chemistry
Indian Institute of Technology Hyderabad
Ordinance Factory Estate,
Yeddumailaram-502 205, A.P.- India.

-Name and affiliation-
Co-Adviser

-Name and affiliation-
Chairman

Acknowledgement

I would like to express gratitude to my project supervisor Dr. D. S. Sharada for her perpetual guidance, fervency and support throughout the project.

I sincerely thank the Department of Chemistry of IIT Hyderabad for providing basic infrastructure and facilities. I would like to thank Dr. M. Deepa and all faculty members of the department for their timely assistance whenever required and encouragement. I thank Ms. Srilaxmi M. for her help and guidance which helped a lot in my project. I also wish to thank research scholars Mr. Anand H. Shinde Mr. Sindhe Vidyacharan, Mr. Arepally Sagar, Mr. Nagarjuna and Mr. Murgan for their constant help, encouragement and valuable suggestion during my lab work. I also like to thank my classmate Ms. Amreen Bains. I extend this opportunity also to thank all my lab mates for their cooperation. I specially remember my friends Argha, Manodeep for their love and company which I will never forget throughout my life.

I wish to express deep gratitude to my parents for their eternal love, support and encouragement.

Last but not the least I wish to thank the almighty for giving me this beautiful life so that I can enjoy his enchanting creation through the path of science.

Kuntal Pal

Dedicated
to
My Parents

Abstract

New organic dyes containing Indole and Carbazole moieties, respectively, as the electron donors, and Barbituric acid, N-acyloxindole moieties as the electron acceptors/anchoring groups have been synthesized and characterized. The influence of heteroatoms on Indole, Carbazole as a donor and the carbonyl-substitution on Barbituric acid and N-acyloxindole as an acceptor is evidenced by spectral, electrochemical,and density functional theory calculations.

Contents

1. Introduction

"More energy from sunlight strikes Earth in 1 hour than all of the energy consumed by humans in an entire year."[1]

The raising of population in the world provokes the energy concerns in every field. ExxonMobil report says that, the energy required per day in 2005 was about 210 million oil-equivalent barrels. This figure rose to more than 300 million oil-equivalent barrels per day currently, with a growing rate of 42.8% compared to the year of 2005. In 2007 Energy information Administration calculate approximately that main sources of energy consisted of petroleum 36.0%, coal 27.4%, and natural gas 23.0%, totaling to an 86.4% contribute to fossil fuels in primary energy burning up in the world.[2] The limited amount of fossil fuel resources and the effects of CO_2 releases on the environment are the two main aspects for the research into renewable energies like sunlight, rain, wind, geothermal heat, and tides. Energy from the sun is the major one of these sources. Yearly the sun could supply the earth with $3 \cdot 10^{24}$ Joules of energy, which is about 10000 times more than the currently global consumptions.[3] The idea to harvest the sunlight and transfer it into electric energy or to produce chemical fuels, such as hydrogen, has in the last couple of decades become reality. In order to be as efficient as possible a solar cell must be able to make efficient use of the solar spectrum (Figure 1.1). The region between 400 and 1100 has the highest photon density in the AM 1.5 solar spectrum. A material that can absorb sunlight between 400 and 1000nm would be the ideal absorber.

For the direct conversion of solar energy into chemical or electrical energy, colloids and nanocrystalline films of several semiconductor systems have been used and they are well developed. The conventional photovoltaics made of crystalline or amorphous silicon are exceptional converter of solar energy to electrical energy with efficiencies of approximately 20%[4] and multijunction solar cells have achieved efficiencies of up to ≈40%.[5] But the main problem is that, the fabrication of these photovoltaics is expensive and energy intensive process.

CuInSe and CdTe thin film photovoltaic cells are the other devices that efficiently convert solar energy to electricity and their efficiency is reached upto 15%.[6] But the small amount of indium,

selenium and tellurium in the earth crust can be a disadvantage for major productions of these cells; also the high toxicity of cadmium is an another drawback. In 1991 O'Regan and Grätzel published an alternative way for harvesting solar energy. They introduced a device based on a mesoscopic inorganic semiconductor, can convert 7% of solar energy to electricity at a low cost.[7]And up to now 13% efficiencies have been achieved with a theoretical efficiency ≈31%.[7] So, globally research is going on to reach as nearer as possible to the theoretical value and to make the solar cell cheaper.

1.1 The dye-sensitized solar cell

A better substitute to multijunction and silicon based solar cells are dye sensitized solar cells (DSSC). DSSCs have the potential to be far cheaper and more efficient than crystalline silicon and multijunction solar cells, primarily due to their abundant use of inexpensive materials.

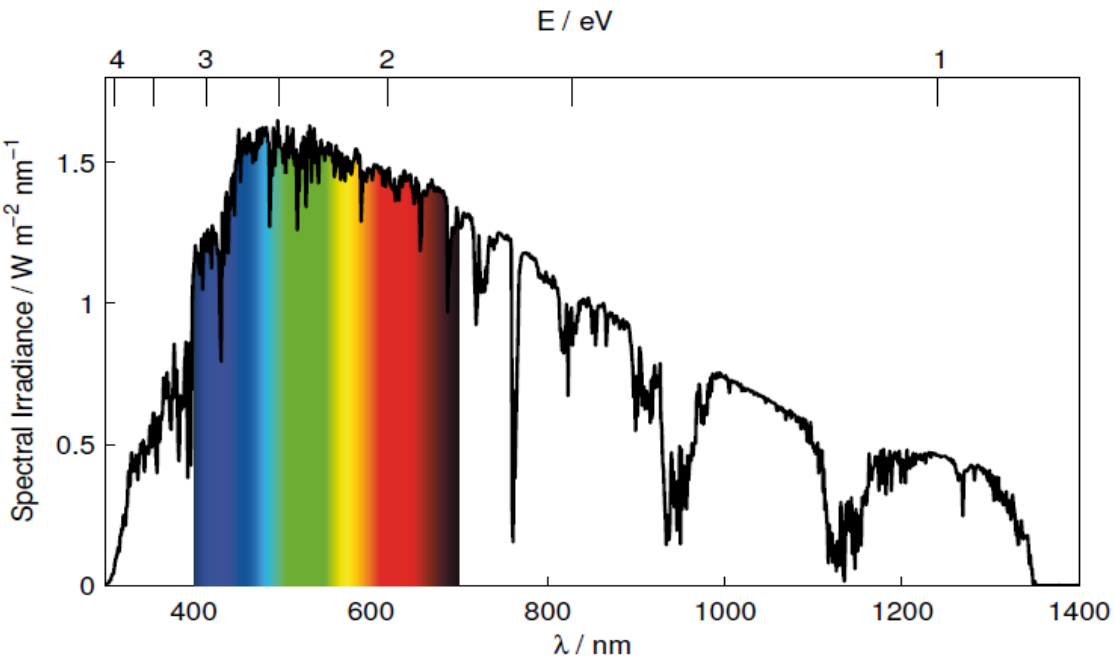

Figure 1.1: Spectral irradiance on the surface of Earth at air mass AM 1.5 conditions, which is the amount of solar radiation that strikes the Earth after passing through one and a half atmospheres. This corresponds to a solar zenith angle of 48.2^{o}

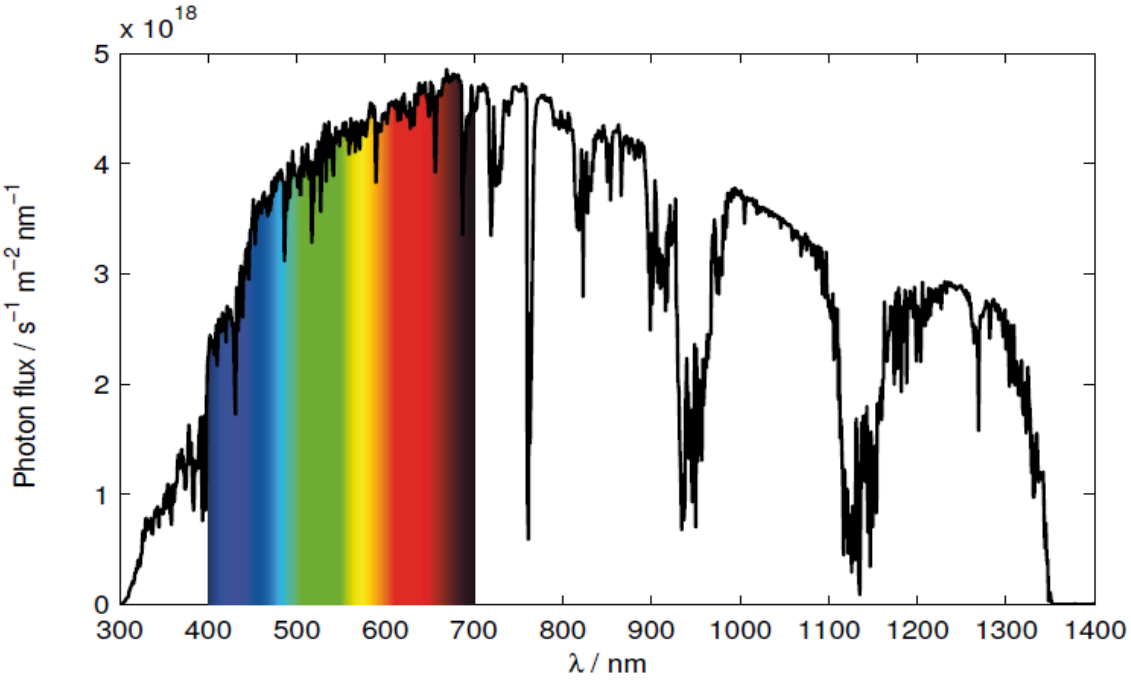

Figure 1.2: Photon flux at the surface of the earth with the visible part of the solar spectrum indicated by its colors.

1.2 Advantages of DSSC

Although the energy conversion efficiency of DSSC is not as good as compared to other inorganic 1st and 2nd generation solar cells, it has an edge over them at some points.

I. DSSC efficiency is nearly temperature-independent in the normal operating temperature range of 25–65°C. For the same range, the efficiency of Si solar cells declines by 20%.[8]

II. DSSC shows even better efficiency than polycrystalline Si solar cell in diffuse sunlight or cloudy conditions. A solar tracking mechanism is less necessary as performance is less sensitive to the incident angle of the light radiation.

III. Although a large commercial production of DSSC is still not available, it can be expected that it has a cost advantage over all thin film devices. Only low cost and abundantly available materials are needed for making DSSC. Unlike amorphous silicon, CdTe or

CIGS cells, DSSC can avoid the costly and energy-demanding high vacuum as well as materials purification steps.

IV. The materials of DSSC are biocompatible and easily available. The technology can be expanded up to the terawatt scale without facing material supply problems. This gives organic dye-based solar cells an advantage over the 2 major competing thin-film photovoltaic technologies - CdTe and CuIn(As)Se; which use highly toxic materials and having small natural abundance.

V. An important requirement for all types of solar cells is long-term stability. From different extensive studies, it has been confirmed that the DSSCs can satisfy the stability requirements for commercial solar cells to bear outdoor operation for 20 plus years.

Considering these advantages, DSSC has the potential to be a feasible candidate for the race of large-scale solar energy conversion systems.

1.3 Basic Operating Principle

The Dye Sensitized Solar Cell (DSSC) follows the same basic principle as plant photosynthesis to generate electricity from sunlight. Each plant leaf is a photo-chemical cell that converts solar energy into biological material. Although only 0.02-0.05% of the incident solar energy is converted by the photosynthesis process, the food being produced is 100 times more than what is needed for mankind.[9] The chlorophyll in green leaves generate electrons using the photon energy, which triggers the subsequent reactions to complete the photosynthesis process.

The DSSC (a typical configuration is shown in Fig. 1.3a,b) is the only photovoltaic device that utilizes separate mediums for light absorption/carrier generation (dye) and carrier transport (TiO_2 nano-particles). The operation steps are the following.

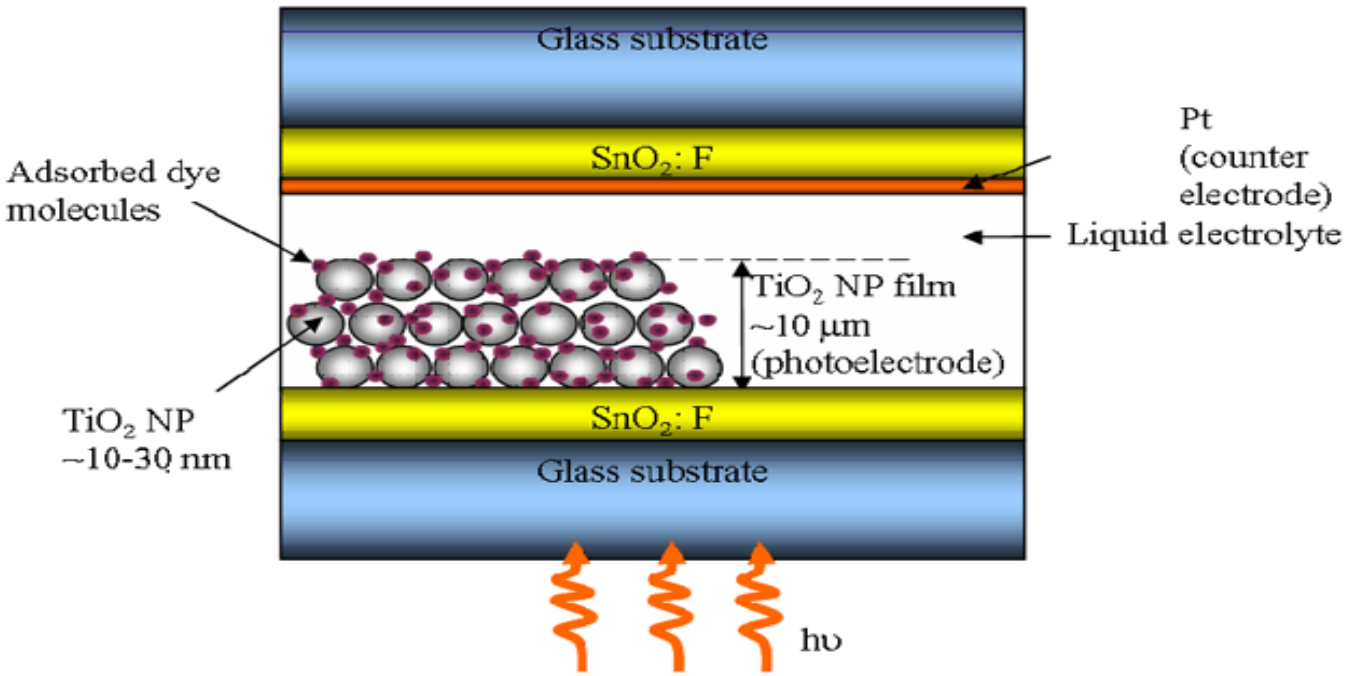

Figure 1.3a: Basic device structure of DSSC

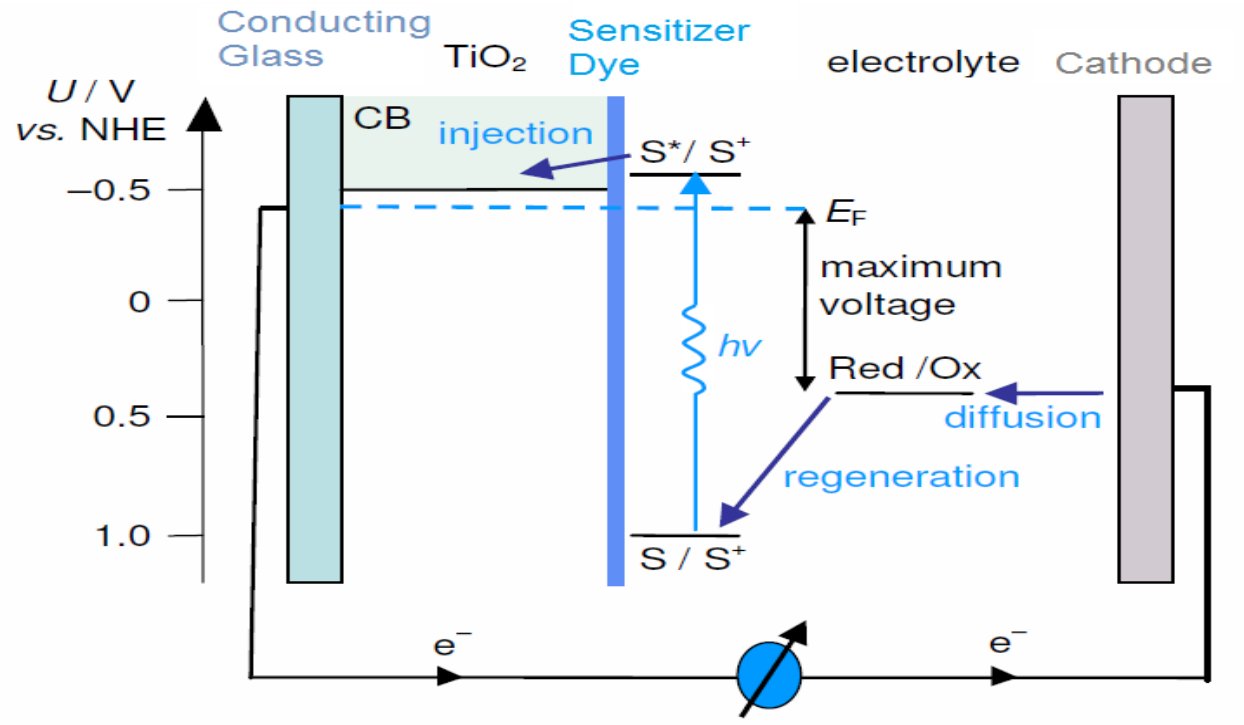

Figure 1.3b: relative band diagram and basic principle for DSSC

1.3a Excitation

The light is absorbed by a sensitizer dye molecule, it goes over an electronic state change from the ground (S) to the excited state (S*). The lifetime of the excited state is in the order of nanoseconds.

$$S + h\vartheta \rightarrow S^* \quad (1.1)$$

$$S^* \rightarrow S^+ + e^- \quad (1.2)$$

1.3b Injection

The sensitizing dye molecules are adsorbed on the surface of a wide band gap semiconductor (typically TiO_2). After the absorption of a photon (excitation), the dye gains the ability to transfer an electron to the conduction band of the semiconductor. The internal electric field of the nanoparticles causes the electron extraction and the dye becomes oxidized (S^+). For efficient electron injection the lowest unoccupied molecular orbital (LUMO) of the dye has to be about 0.3 eV above the TiO_2 conduction band. The injection rate constant is in the femtosecond range for singlet state.

1.3c Diffusion in TiO_2

The nonporous TiO_2 film consists of spherical anatase particles of diameter ~20 nm. The presence of oxygen vacancies in the lattice makes it a weakly n-doped material (equivalent carrier concentration 10^{16} cm^{-3}).[10] As the TiO_2 particle diameter is too small for electric field to build up, the dominant electron transport mechanism is diffusion via trapping and de-trapping.

1.3d Iodine Reduction

The electron travels through the outer circuit performing work, reaches the back FTO electrode, and reduces the iodine in the electrolyte. The platinum layer on the FTO acts as a catalyst for the reduction. The dark cathode reaction:

$$I_3^- + 2e^- \rightarrow 3I^- \quad (1.3)$$

The iodine reduction can also occur at the excited dye molecules causing recombination of the photo-generated electrons. For efficient charge transfer, the rate of iodine reduction at the counter electrode has to be more rapidly than the recombination at the TiO_2/electrolyte interface.

1.3e Dye Regeneration

The reduced iodide ion replenishes the highest occupied molecular orbital (HOMO) of the dye - regenerating its original form, and makes it ready for electron generation again. The photoanode reaction:

$$2I^- \rightarrow I_2 + 2e^- \qquad (1.4)$$

This prevents buildup of S^+, which could lead to the conduction band electrons going back to the dye molecules. The maximum output voltage equals to the difference between the Fermi level of the semiconductor and the redox potential of the mediator.[11] Thus, the device is can produce electricity from light without undergoing any permanent physical and chemical change.

Therefore the overall reactions going in a dye sensitized solar cell is as follows, [12]

Reaction Equation	**Event Description**
$\mathbf{S + photon \rightarrow S^*}$	Photo excitation
$\mathbf{S^* \rightarrow S^+ + e^-_{(TiO_2)}}$	Charge injection
$\mathbf{S^+ + 2I^- \rightarrow S + I_2^{\bullet -}}$	Dye regeneration
$\mathbf{2\ I_2^{\bullet -} \rightarrow I_3^- + I^-}$	Dye regeneration
$\mathbf{I_3^- + 2e^- \rightarrow 3I^-}$	Electrolyte regeneration
$\mathbf{S^* \rightarrow S}$	Dye relaxation
$\mathbf{S^+ + e^-_{(TiO_2)} \rightarrow S}$	Recombination via dye
$\mathbf{2\ e^-_{(TiO_2)} + I_3^- \rightarrow 3I^-}$	Recombination via electrolyte

1.4 Metal and Metal-Free Dipolar Organic Dyes

As one of the most vital factors that control the performance of DSSC, the sensitizing dyes engage various types of molecules from synthetic metal complexes to natural dyes. Also, incredible new artificial metal-free organic dyes have been synthesized and utilized as the sensitizer in DSSCs. Among them Ru(II)-based complex dyes remain leading in photoelectronic conversion efficiency of solar energy. However, the difficult purification and elevated cost of Ru-based dyes bound their progress compared to the metal-free organic dyes. Although none of the pure organic dyes has greater photoelectronic conversion efficiency than the Ru-based sensitizers presently, there is quick development and a rising attention for the growth of metal free organic dyes showing efficient charge separation and wide spectral response due to their impending application as sensitizers in the dye-sensitized solar cells (DSSCs). Up to now, the metal-free organic sensitizers have achieved promising solar energy-to-electricity conversion efficiencies (η) comparable to Ru-based complexes.[13]Huge studies have been allocated to design novel metal free structural dyes, to explain the connection between the structure and properties and to optimize the DSSC devices. Also some efforts have been allocated to optimize the functional properties such as absorption, intra-molecular charge transfer and redox stability by simple molecular engineering.

Many metal-free organic based dyes have been used in DSSCs, such as, coumarin, merocyanine, indoline, polyene, hemicyanine, triphenylamine, fluorene, carbazole and phenothiazine.[14] Usually, metal-free organic dyes acquire the apparent molecular structure of the electron donor part, acceptor part bridged by the conjugated chain (D-π-A) and an anchoring unit for binding to the semiconductor surface.

In the present situation both at national and international level the scientific community has turned their attention to develop organic dyes for efficient solar energy harvesting by tuning the different sections (donor part, acceptor part, the conjugated π chain (D-π-A) and anchoring moiety) of general molecular structure of the dye.[15] To date 13% is the highest efficiency reported for organic dyes in DSSC. In spite of these developments, there is a demand for developing highly efficient and durable dye. With this perspective, we plan to design and develop a series of novel metal-free dyes with higher photovoltaic performance in DSSCs.

1.5 Basic Structure of the Metal-Free Dipolar Organic Dyes

A general way of proposing organic dyes is the D-π-A approach, where the molecule is built up of an electron donor, a π-spacer, and an electron acceptor, as demonstrated in Figure 1.4. This particular structure will capitulate an intramolecular charge transfer upon excitation which is required for DSSCs. Since in the preface of DSSCs, variety of structures have been used as organic sensitizers such as indoline, perylene, coumarine and carbazole.[16] 2-cyanoacrylic acid is the most frequently used acceptor that unites the electron withdrawing nature of the cyano group with the anchoring carboxylic acid group. Phosphonic acid, silanol, hydroxamate and barbituric acid are the examples of other anchoring groups. The policy of our work has been to alter one of these divisions separately, in order to gain more efficiency by changing different sections contributing to the overall performance.

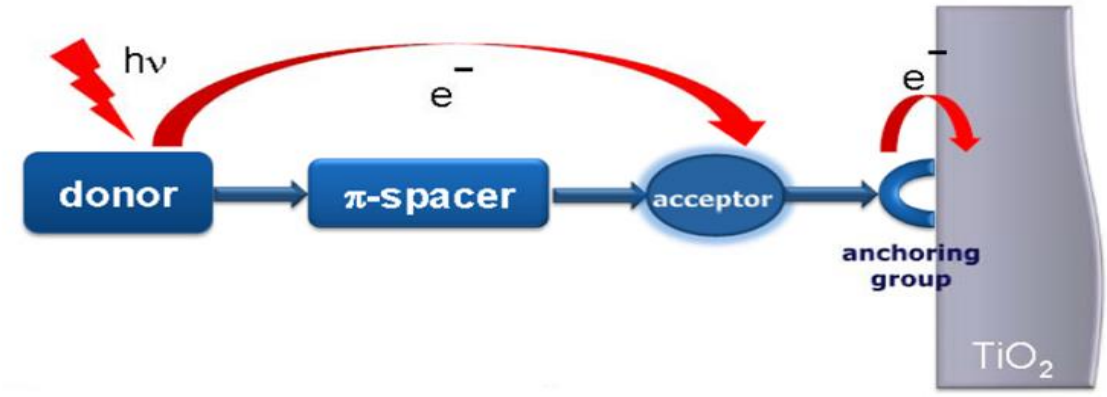

Figure 1.4: Illustration of a sensitizer with the Donor-Linker-Acceptor design

If we expand the σ* conjugation in the dyes and introduce an electron-donating and –withdrawing substituents into the dye scaffold the absorption spectra of organic dyes could be red-shifted. The levels of highest occupied molecular orbitals (HOMOs) and lowest unoccupied molecular orbitals (LUMOs) of the dyes can be shifted by such substituents. Red-shifting the absorption band is not the only key factor in the plan of capable organic-dye photo-sensitizers; the potential energy levels of the HOMO and LUMO must be in proper positions when compared to the conduction band level of the semiconductor electrode and to the iodine redox potential. A red shift in the absorption spectrum decreases the energy gap between the HOMO

and the LUMO of the dye. The HOMO level must be more positive than the iodine redox potential to accept electrons, and to inject electrons, the LUMO level must be more negative than the conduction band level of the semiconductor.[17]

Alternatively donor–acceptor (D–A) conjugated organic molecules are also a significant organic materials, and have fascinated much educational and scientific research interest[18]. In these type of compounds the electron-donating and electron-accepting groups are linked through a π-conjugated bridge. Regulating different donor part or acceptor part in a D–A molecule would alter its physical and chemical properties.

2. Results and Discussion

2.1. Synthesis and Structure of Sensitizers

As shown in Figure 2.1, **D1** and **D2** are barbituric acid-based dyes with indole and carbazole unit as the donor, respectively. **D3** is N-acyl oxindole based dye with carbazole as a donor group.For preparing these dyes first N-methylation of indole and carbazole is done by using methyl iodide in presence of sodium hydride in DMF.[19] Next the aldehydes **3**, **6** are prepared by a Vilsmeier reaction of N-methylindole and *N*-methylcarbazole, respectively, with $POCl_3$ in DMF.[20] Then the final reaction for **D1** and **D2** is the condensation of the respective aldehyde with barbituric acid by the Knoevenagel condensation reaction in the presence of methanol as a solvent. The dye **D3** is prepared by the Knoevenagel condensation reaction of N-methylcarbazole with oxindole in presence of pipyridine in ethanol, followed by the N-acylation of the oxindole moiety with acetic anhydride in presence of sodium hydride in DMF.

(D1)

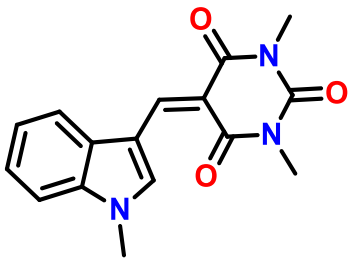

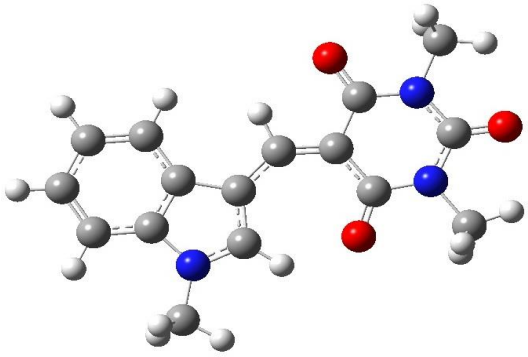

(D2)

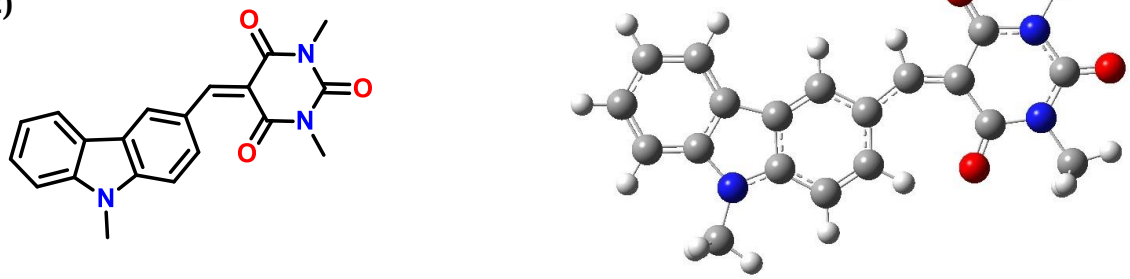

(D3)-Z

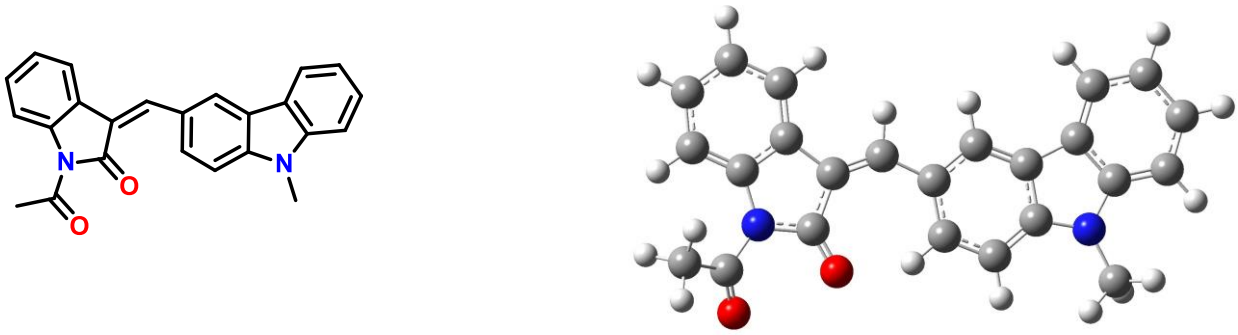

(D3)-E

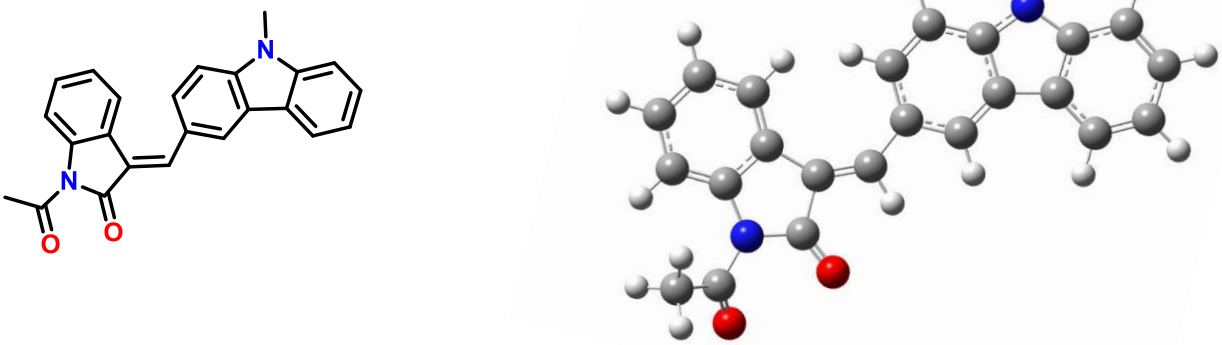

Figure 2.1: Optimized structure of D1, D2 and D3

2.2. Synthetic Procedure of Indole and Carbazole-containing Dyes D1–D3

(D1)

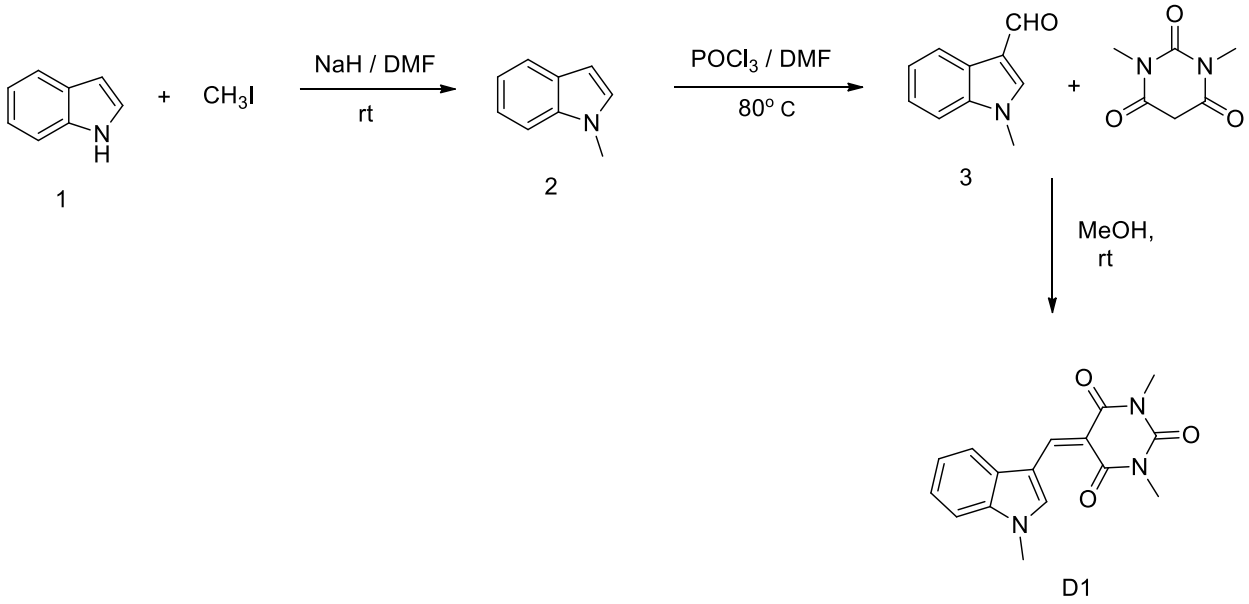

(D2)

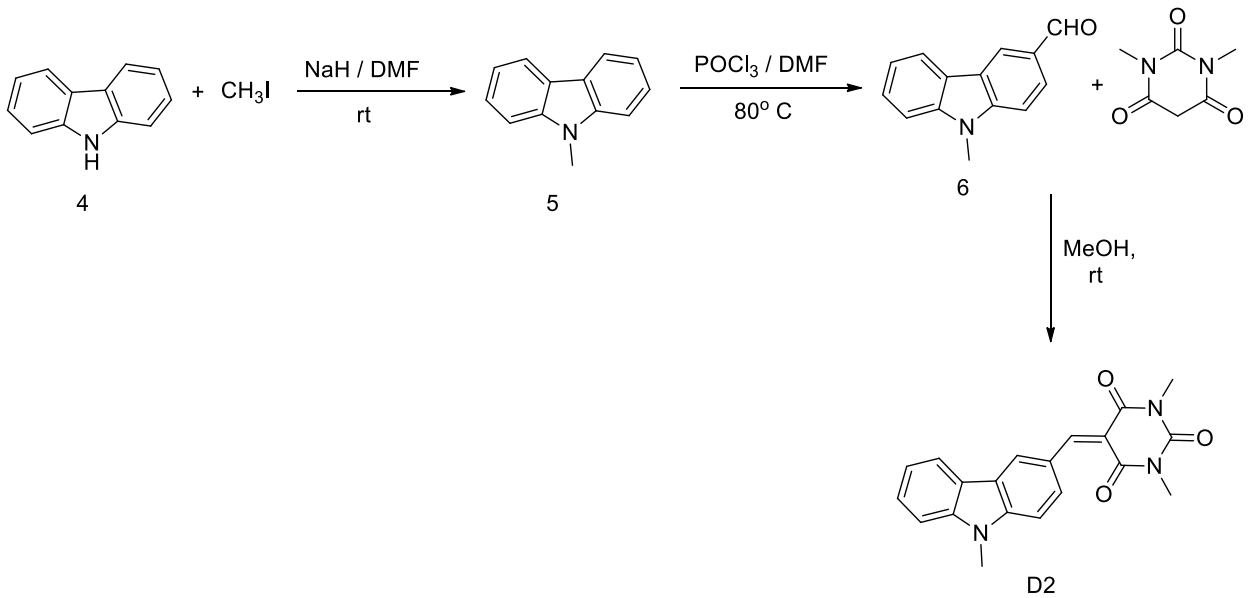

(D3)

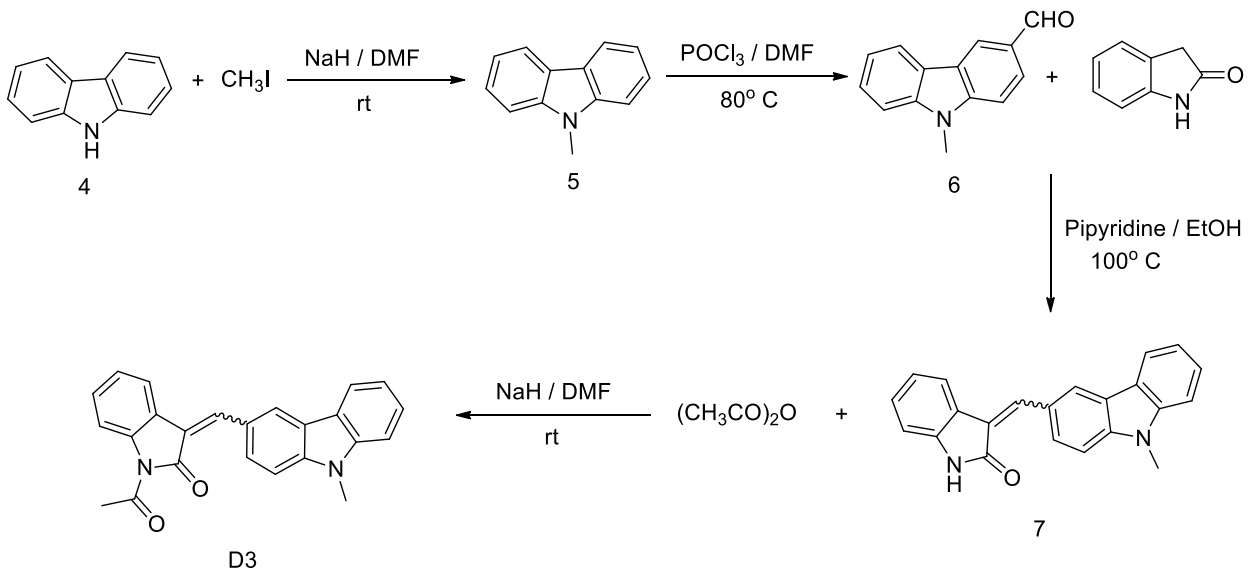

Figure 2.2: Synthesis of the dyes **D1**–**D3**.

2.3. Molecular Orbital Calculations

The geometrical and electronic properties of **D1**–**D3** are examined by time dependent density functional theory (TD-DFT) using the Gaussian 09 program package, as shown in Figure 2.3. The calculations are done by using B3LYP/6-31G(d) level for geometry optimizations in the ground state. B3LYP is a hybrid function which is modified from the three-parameter exchange-correlation functional of Becke[21], while the gradient-corrected exchange and correlation functions are determined according to Becke[22] and Lee *et al*.[23] The frontier MOs of **D1** and **D2** reveal that HOMO–LUMO excitation moves the electron density distribution from the indole and carbazole moiety to the barbituric acid moiety. Comparing the frontier MOs of **D1** and **D2** at the ground state (HOMO), the electron density in **D1** is homogeneously distributed in all aver the molecules whereas in **D2** the electron density is mainly over carbazole moiety. While going from HOMO to LUMO a little amount of electron density is shifted from indole moiety to the methylene bridge and barbituric acid part of **D1**, but a large electron density shift is observed

from carbazole moiety to methylene bridge and barbituric acid part in **D2**.Similarly in case of both **D3 (E)** and **D3 (Z)** the electron density is shifted from donor carbazole part to acceptor oxindole moiety while going from HOMO to LUMO. However in HOMO-1 the electron density is mainly located over the barbituric acid group of both **D1** and **D2,** and over oxindole group in **D3.** And in LUMO+1 electron density is centered on indole and carbazole unit of **D1**, **D2** and **D3** respectively. Furthermore, the location of the LUMO at the side of the TiO_2 surface and the HOMO at the opposite end of the molecule makes the electron injection into the semiconductor easier and prevents back regeneration of the dye with injected electrons. Highest occupied molecular orbital (HOMO), lowest unoccupied molecular orbital (LUMO) are calculated to find ΔE (Energy gap) are given in Table 2.1.

Table 2.1: HOMO LUMO energy calculated by DFT method (eV)

Dyes	**B3LYP/6-31G(d) (eV)**		
	HOMO	**LUMO**	**Energy gap (LUMO-HOMO)**
D1	-5.7530	-2.0381	3.7149
D2	-5.7288	-2.2147	3.5141
D3(E)	-5.5794	-1.8901	3.6893
D3(Z)	-5.7136	-2.0542	3.6593

Table 2.2: Excitation energies (eV, nm), Oscillator strengths (*f*), Assignment of molecular orbital contributions, Dipole moment of the dyes calculated by TD-DFT

Dye	**Excited State**	**Oscillator Strength (*f*)**	**Excitation energy ΔE (eV)**	**Excitation energy ΔE (nm)**	**Composition H=HOMO, L=LUMO**	**μ_g (debye)**
D1	1	0.6258	3.4917	355.09	0.70245×(H→L)	5.9471
	2	0.0000	3.5573	348.53	0.69600×(H-2→L)	
	3	0.0238	3.9159	316.61	0.69481×(H-1→L)+ 0.11348×(H→L+1)	

D2	1	0.5721	3.2356	383.19	-0.22243×(H-1→L)+ 0.66490×(H→L)	5.9875
	2	0.2197	3.4303	361.44	0.65332×(H-1→L)+ 0.22020×(H→L) -0.13238×(H→L+1)	
	3	0.0000	3.4711	357.19	0.69635×(H-2→L)	
D3(E)	1	0.7727	3.4063	363.99	0.64101×(H→L)	7.1735
	2	0.0035	3.6646	338.33	0.64656×(H-1→L) - 0.24135×(H→L+1)	
	3	0.0103	3.7752	328.42	-0.13949×(H-6→L)+ 0.59286×(H-3→L) - 0.29554×(H-2→L)	
D3(Z)	1	0.0020	3.0630	404.77	0.67057×(H-2→L)	4.4037
	2	0.3809	3.3264	372.73	-0.33176×(H-1→L)+ 0.58475×(H→L)	
	3	0.2979	3.4076	363.85	0.59812×(H-1→L)+ 0.29245×(H→L)	

2.3.1. Light Harvesting Efficiency (LHE) and Oscillator Strength (*f*):

The light harvesting efficiency (LHE) is the efficiency of dye to response the light. It is another important factor for DSSC which indicates the efficiency of the dye. With increasing light harvesting efficiency the photo-current response of the dye is maximized.

The oscillator strength is directly calculated from TD-DFT method. We have calculated the LHE of the main absorption peaks by using the formula 2.1 [24] as shown in Table 2.3.

$$LHE = 1\text{-}10^{-f} \qquad (2.1)$$

Table 2.3: Light Harvesting Efficiency (LHE) of **D1-D3**

Dyes	Gas phase			
	Excitation energy ΔE (eV)	**λ_{max} (nm)**	**Oscillator Strength (f)**	**LHE**
D1	3.4917	355.09	0.6258	0.7633
D2	3.2356	383.19	0.5721	0.7321
D3(E)	3.4063	363.99	0.7727	0.8312
D3(Z)	3.0630	404.77	0.0020	0.0046

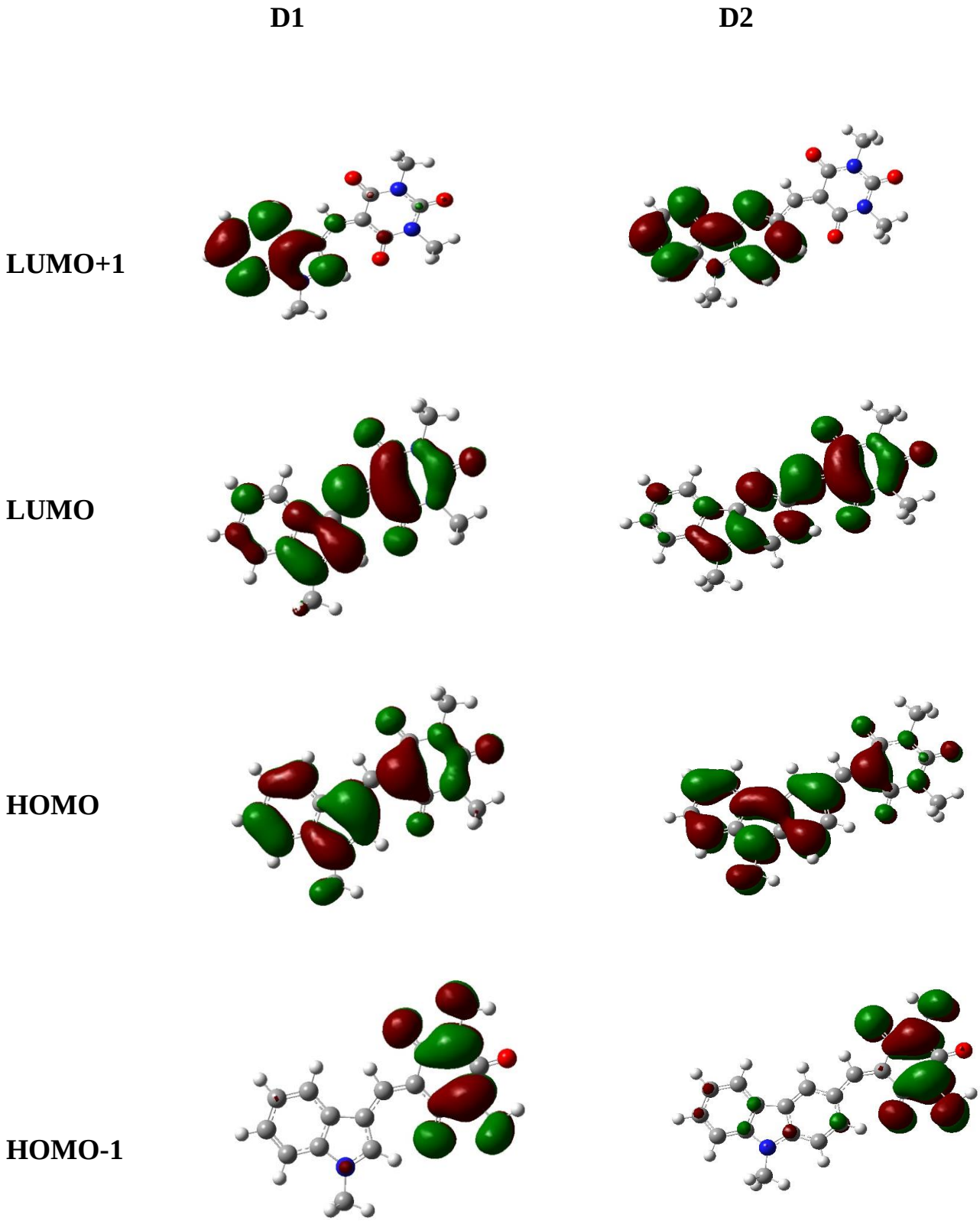

Figure 2.3: Computed isodensity surfaces of HOMO and LUMO orbitals of **D1**and **D2**

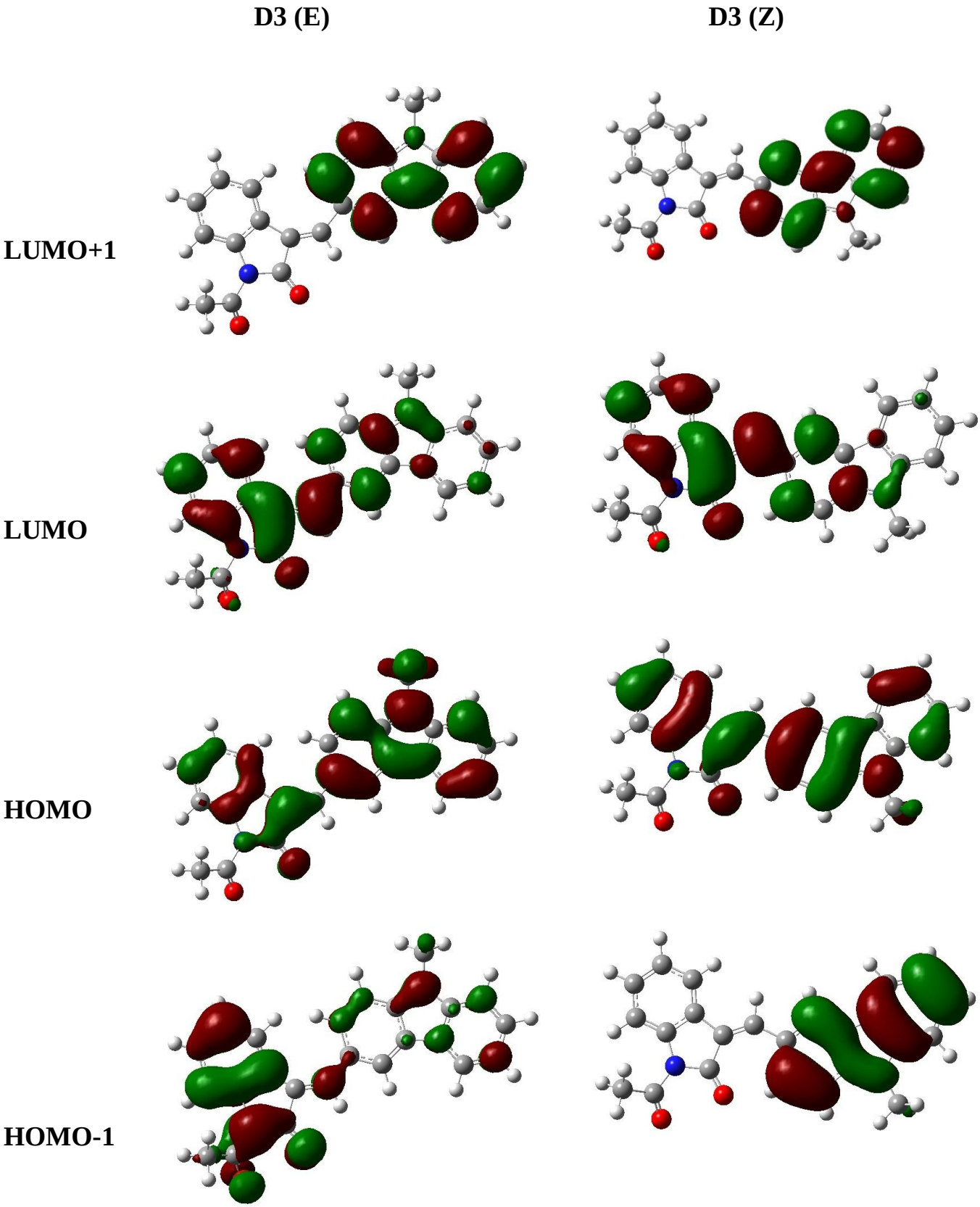

Figure 2.3: Computed isodensity surfaces of HOMO and LUMO orbitals of **D3 (E)** and **D3 (Z)**

2.4. Optical Properties of the Dyes:

Figure 2.5 shows the UV-Vis absorption spectra for the three dyes in DCM and the λ_{max} are listed in Table 2.4. The absorption spectrum of **D1** in DCM has three distinct absorption bands at around 318 and 456 nm, respectively. The absorption peaks at around 318 nm correspond to the $\pi \rightarrow \pi^*$ electron transition of the conjugated molecule; and the absorption peaks at around 456 nm can be assigned to an intramolecular charge transfer between the indole-based donor and the barbituric acid, providing efficient charge-separation at the excited state. Under similar conditions, the **D2** sensitizer had absorption peaks at 358 and 492 nm that were red-shifted relative to the peaks of **D1**, implying that the incorporation of one more phenyl ring increases the conjugation in **D2.** Compare the maximum absorption wavelength of **D1**–**D3** in DCM solution. **D3** (562 nm) shows a red shift relative to **D1** (456 nm) and **D2** (492 nm), which can be attributed to the extra conjugation present in **D3**. Such red-shifting in the absorption spectra implies a more effective utilizing of solar light. But **D3** has the less absorption among the three dyes. Again as D3 is a mixture of E and Z, we got a broad absorption peak.

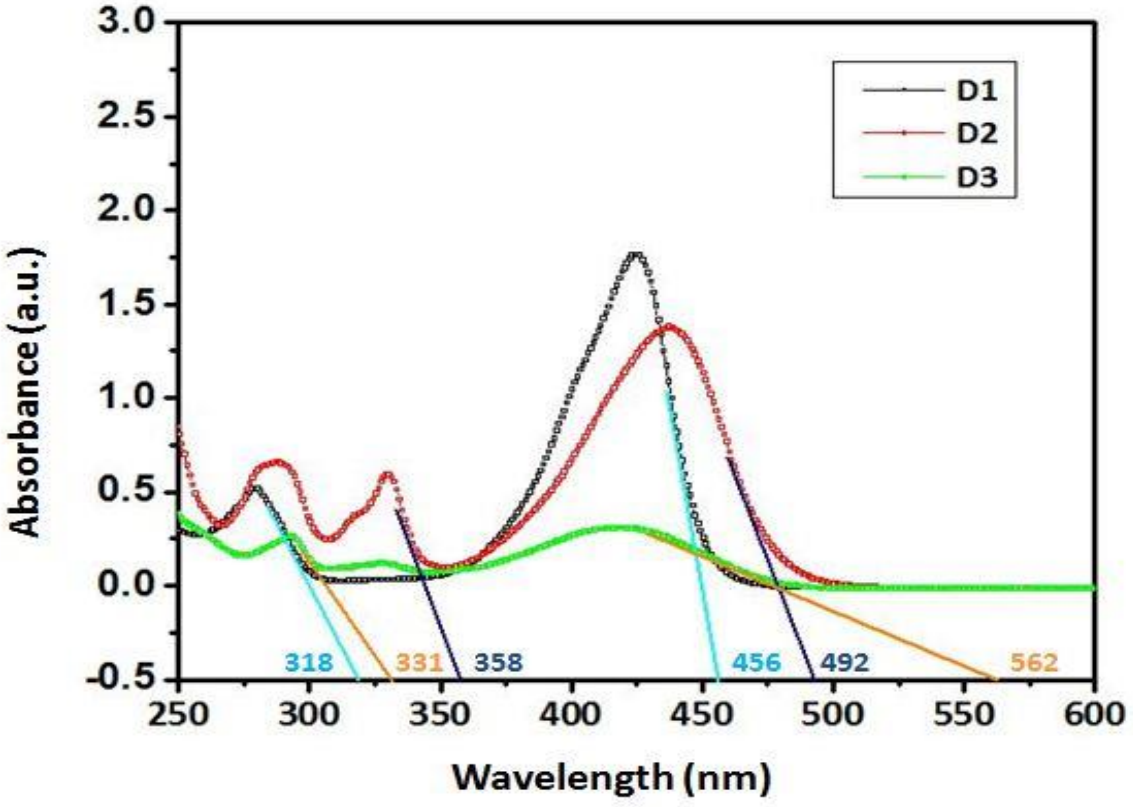

Figure 2.5: Absorption spectra of **D1**–**D3** in DCM

Table2.4: Absorption properties (λ_{abs}) of dyes.

Dyes	λ_{abs}(nm) in DCM
D1	318, 456
D2	325,358, 492
D3	331, 562

2.5. Electrochemical Properties of the Dyes:

To judge the possibilities of electron transfer from the excited dye molecule to the conductive band of TiO_2 and the dye regeneration, redox potentials of **D1**–**D2** in dichloromethane were obtained using cyclic voltammetry (as shown in Figure 2.6). The electrochemical data are listed in Table 2.5. The excited-state oxidation potentials were obtained from the first oxidation potential Eox (*vs.* NHE) measured by cyclic voltammetry, Ag/AgCl/KCl redox couple was used as an internal potential reference.

(a)

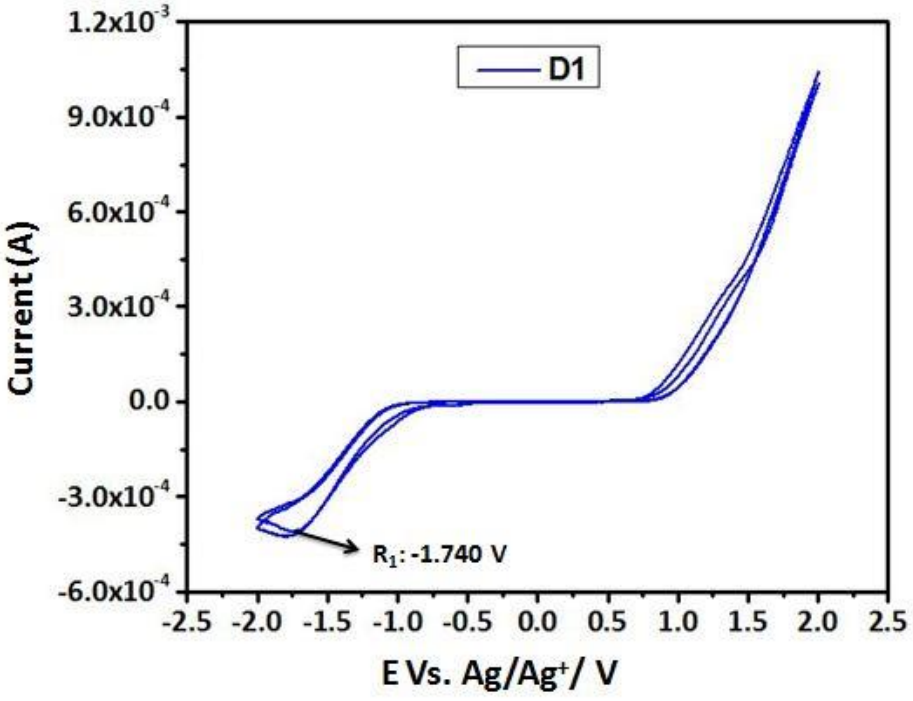

(b)

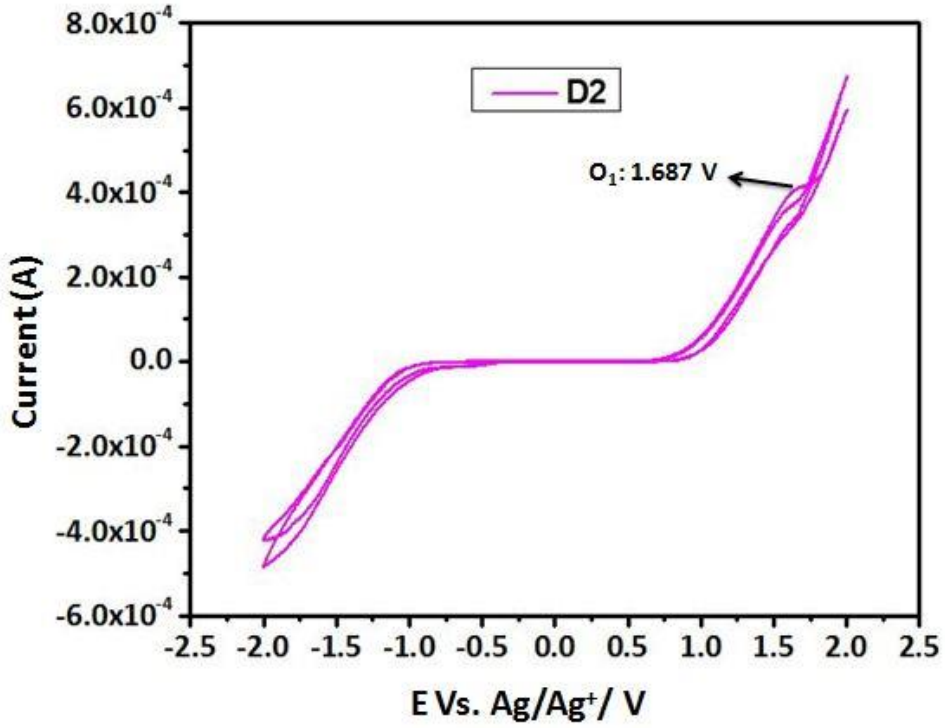

(c)

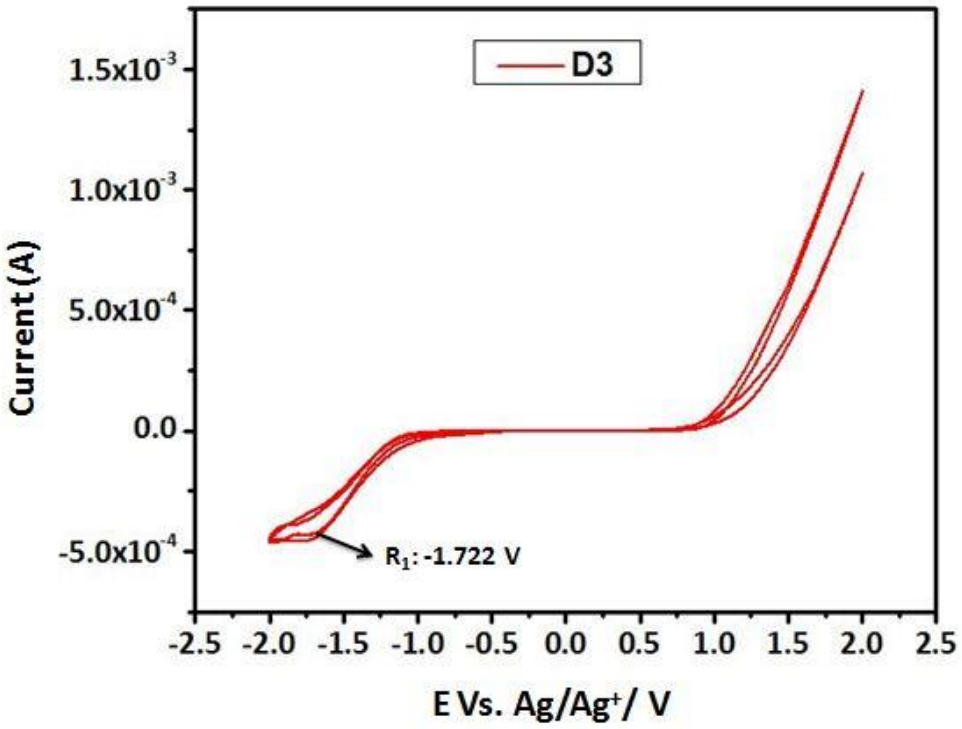

.

Figure 2.6: Cyclic voltammograms recorded at a scan rate of 100 mVs-1 in a 0.1 M tetrabutyl ammonium iodide solution in two electrode electrochemical cells with Ag/AgCl/KCl as reference electrode and a Pt rod as the auxiliary electrode (a) **D1** in DCM/FTO plates as both electrodes, (b) **D2** in DCM/FTO plates as electrodes (c) **D3** in DCM/FTO plates as electrodes,

The cyclic voltammograms of **D1** and **D3** show the first reduction peak (labeled as R1 for each electrode in Figure 2.6) at –1.740 and –1.722 V (versus Ag/Ag+) in their cathodic branches respectively. The potential of reference electrode (Ag/Ag+) was +0.197 V (versus NHE)[25]. The reduction potential (versus NHE) corresponds to the LUMO of the electroactive dyes.

Therefore, the reduction potential of **D1** (versus NHE) will be: E_R = (–1.740 + 0.197) V = –1.543 V. Similarly, the reduction potential of **D3** (versus NHE) will be: E_R = (–1.722 + 0.197) V = –1.525 V. A potential of 0 V (versus NHE) corresponds to 4.5 eV (w.r.t. vacuum level)[25]. The LUMO or CB positions of **D1** and **D3** were therefore calculated to be 2.957 eV and 2.975 eV respectively.

The cyclic voltammograms of **D2** shows oxidation peak (labeled as O1) at 1.687 V (versus Ag/Ag+). The potential of reference electrode (Ag/Ag+) was +0.197 V (versus NHE). The oxidation potential (versus NHE) corresponds to the HOMO of the electroactive dyes. Therefore, the oxidation potential of **D2** (versus NHE) will be: E_O= (1.687+0.197) V= 1.884 V. A potential of 0 V (versus NHE) corresponds to 4.5 eV (w.r.t. vacuum level). The HOMO or VB position of **D2** was therefore calculated to be 6.384 eV.

Table 2.5: Electrochemical data of **D1** and **D2**

Dyes	**LUMO**		**Absorbance from UV-Vis**		**HOMO**	
	w.r.t. NHE (V)	**w.r.t. vacuum (eV)**	**in nm**	**in eV**	**in eV**	**in V(w.r.t. NHE)**
D1	–1.543	2.957	456	2.719	5.676	1.176
D2	–0.636	3.864	492	2.520	6.384	1.884
D3	–1.525	2.975	562	2.206	5.181	0.681

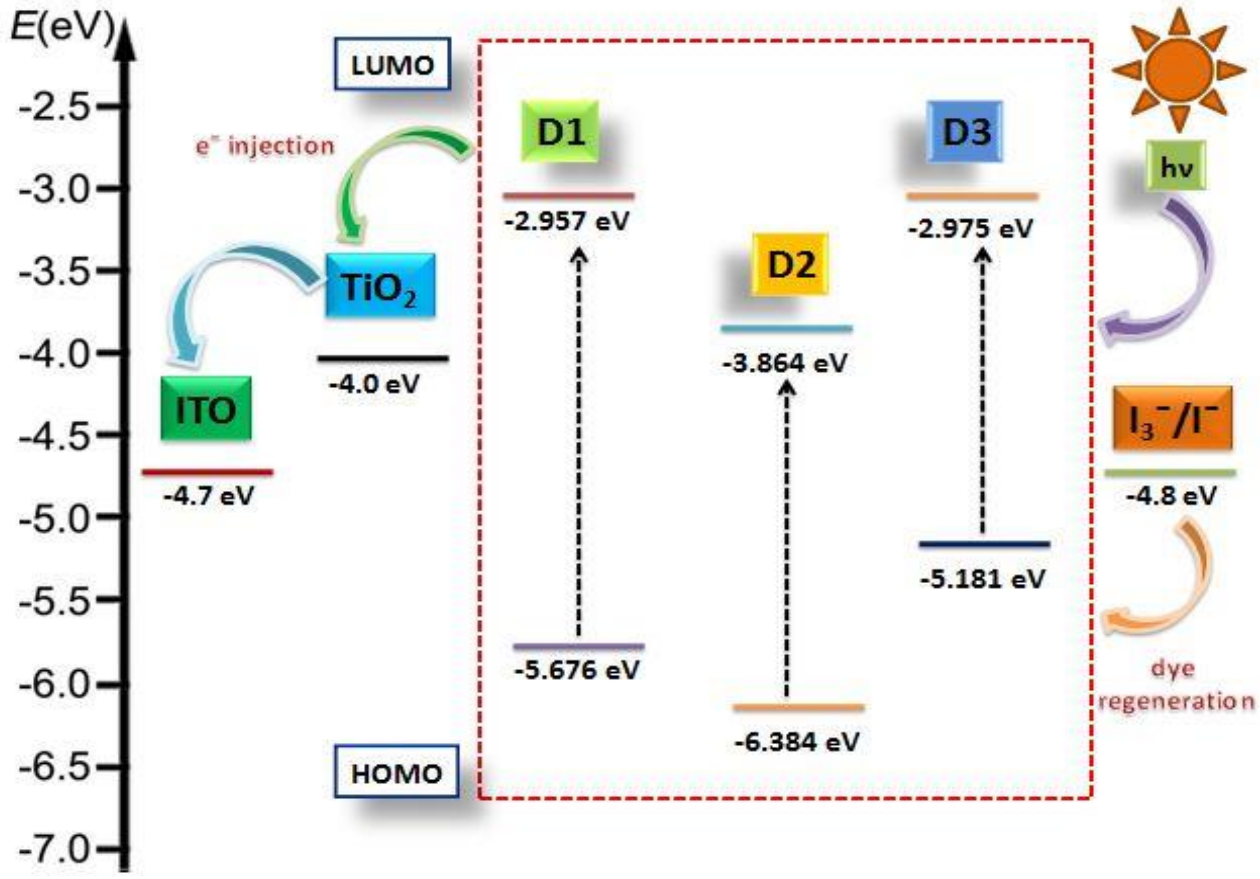

Figure 2.7: Energy levels of the dyes and other materials used for DSSC fabrication.

2.6 Conclusion

In summary three simple dyes having Indole (**D1**) or Carbazole (**D2** and **D3**) moiety as a donor and barbituric acid (**D1** and **D2**) or N-acyl oxindole (**D3**) as acceptor have been designed and synthesised from very cheap starting materials within short period of time. These dyes are characterised by DFT calculation, UV-Vis absorption and cyclic voltametry. Electrochemistry along with DFT calculations revealed that the low-lying LUMO caused by the substitutions is the main reason for the narrowed HOMO-LUMO gaps. The LUMO values of **D1** (–1.543V), **D2** (–0.636V) and **D3** (–1.525V) are more negative than the conduction band edge of TiO_2 [−0.5 V (*vs.* NHE)]. The HOMO values of **D1** (1.176V), **D2** (1.884V) and **D3** (0.681V) are sufficiently

more positive than the I_3^-/I^- redox potential [0.42 V (*vs.* NHE)]. The DFT calculations reveal that HOMO–LUMO excitation moves the electron density distribution from the donor (indole and carbazole) to the acceptor (barbituric acid and N-acyl oxindole). We believe that, these dyes can be used efficiently as a dye for making solar cells. Detailed experiments and the investigation of efficiency and the interfacial charge transfer processes of these dyes are in progress aiming to acquire an excellent outcome of DSSCs fabricated with this new group of dyes.

3. Experimental section

3.1 General information

In this section the preparations of all the compounds that have been made in the course of thesynthesis of tetrazolyl tetrahydroisoquinolines have been discussed.For the experiments, all starting material and reagents are purchased from standard commercial sources or were prepared in the laboratory. All the glasswares were cleaned with soap water followed by acetone and dried in hot air oven at 100 ˚C for 2h.Solvents were distilled prior to use; petroleum ether with a boiling point range 40-60 ˚C was used.

IR spectra were recorded on the Bruker Tensor 37(FTIR) spectrophotometer. ^{1}H NMR spectra were recorded on Bruker Avance 400 (400 MHz) spectrometer at 295K in $CDCl_3$; chemical shifts value (δ ppm) and coupling constants (Hz) are reported in standard fashion with reference to either tetramethylsilane (TMS) (δ-H = 0.00 ppm) or $CHCl_3$ (δ-H = 7.26ppm). ^{13}C NMR spectra were recordedon Bruker Avance 400 (100 MHz) spectrometer at 298K in $CDCl_3$; chemical shifts (δ ppm) are reported relative to $CHCl_3$ [(δ-C=77.00ppm) central line of triplet]. In ^{13}C NMR the nature of carbons (C, CH, CH_2, and CH_3) was determined by recording the DEPT- 135 spectra. In ^{1}H NMR, the following abbreviations were used throughout the thesis; s = singlet, d = doublet, t = triplet, q = quartet, qui = quintet, m = multiplet and br.s = broad singlet. The assignment of the signals was confirmed by ^{1}H, ^{13}C and DEPT spectra. Reactions were monitored by TLC on silica gel (254 mesh) using a combination of petroleum ether and ethyl acetate as eluents.

3.2 Preparation of Starting Material and Dyes

(1) General Procedure for preparation of N-methyl indole (2) and N-methyl carbazole(5)[19]

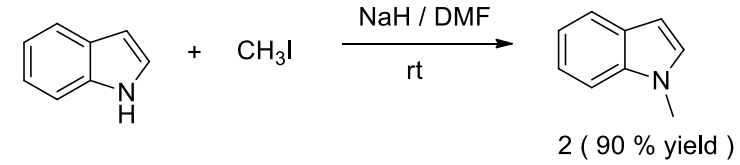

2 (90 % yield)

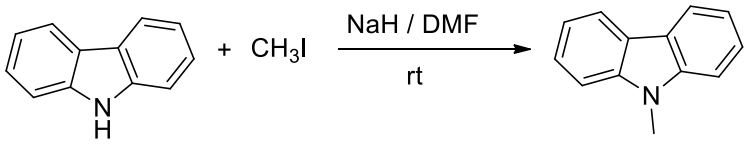

5 (91% yield)

To an ice-bath cooled suspension of washed NaH (1.2 equiv.) in DMF was added dropwise the corresponding indole/carbazole (1 equiv.) at 0°C. The resulting mixture was stirred at 0°C for 30 min. and at room temperature for additional 30 min. After cooling to 0 °C, iodomethane (1.2 equiv.) was added and the solution was stirred at room temperature for 24h. Then a saturated aqueous solution of NH_4Cl was added and the product was extracted with AcOEt. The combined organic phases were washed by water and brine, and dried over Na_2SO_4. The product was then purified by flash chromatography.

(2) General Procedure for preparation of 1-methyl-1H-indole-3-carbaldehyde (3) and 9-methyl-9H-carbazole-3-carbaldehyde (6)[20]

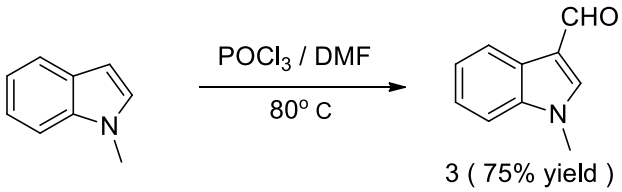

3 (75% yield)

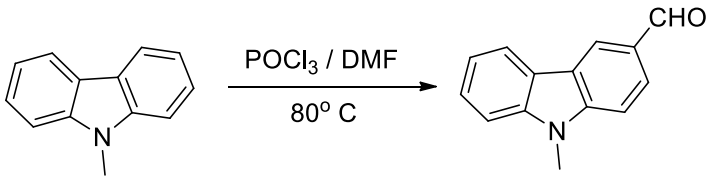

6 (85% yield)

Phosphorous oxychloride (2 mmol) was added dropwise to dimethylformamide (3 mL) cooled under ice-bath and allowed to stir for 30 min. A solution of 1-Methyl-1H-indole (2) or 9-methyl-9H-carbazole (5) (1 mmol) in DMF (5 mL) was added dropwise for 5 min at 0 ^{o} C. The mixture was further allowed to stir for 3 h at 90–100 ^{o} C. Reaction mixture was cooled to room temperature and poured into crushed ice. Excess $POCl_3$ was quenched with 1 N NaOH and left overnight at room temperature. Ice-cold reaction mixture was then extracted (50 mL× 3) with EtOAc. Combined organic layer was concentrated on rotary evaporator and crude products were purified by silica gel column chromatography to get 1-methyl-1H-indole-3-carbaldehyde (3) and 9-methyl-9H-carbazole-3-carbaldehyde (6).

(3) General Procedure for preparation of 1,3-dimethyl-5-((1-methyl-1H-indol-3-yl)methylene)pyrimidine-2,4,6(1H,3H,5H)-trione (D1) and 1,3-dimethyl-5-((9-methyl-9H-carbazol-3-yl)methylene)pyrimidine-2,4,6(1H,3H,5H)-trione (D2)

The 1-methyl-1H-indole-3-carbaldehyde (3) or 9-methyl-9H-carbazole-3-carbaldehyde (6) (1 mmol) and N,N-dimethylbarbituric acid (1.2 mmol) were added to 10 volumes of methanol and the resulting mixture stirred at room temperature. The final product, the appropriate crashed out of the solution once the reaction was complete (1–2 h). The final product was filtered and washed by methanol to afford the dyes (**D1** and **D2**) in excellent yield.

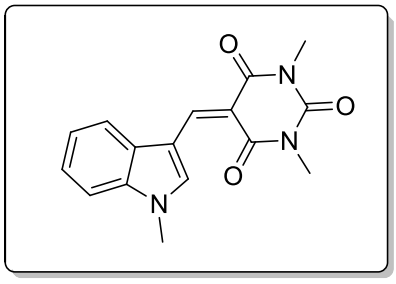

1,3-dimethyl-5-((1-methyl-1H-indol-3-yl)methylene)pyrimidine-2,4,6(1H,3H,5H)-trione (D1): Yellow solid; mp 288-290°C; 95% yield; IR (MIR-ATR, 4000-600cm^{-1}):ν_{max}= 1648, 1556, 1460, 1389, 1388, 1234, 1121, 1068, 784, 741, 645, 529 cm^{-1}; ^{1}H NMR (400 MHz, $CDCl_3$) δ ppm= 3.44(s, 6H), 3.97(s, 3H), 7.44-7.39(m, 3H), 8.02-8.00(m, 1H), 9.01(s, 1H), 9.56(s, 1H); ^{13}C NMR (100 MHz, $CDCl_3$) δ ppm = 28.07, 28.81, 34.32, 108.04, 110.57, 112.06, 118.75, 123.38, 124.16, 130.54, 137.38, 143.12, 146.29, 151.83, 162.32, 163.87; HR-MS (ESI^{+}) *m/z* calculated for $C_{16}H_{15}N_3O_3Na^{+}$ [M + Na^{+}]: 320.10; found: 320.0999.

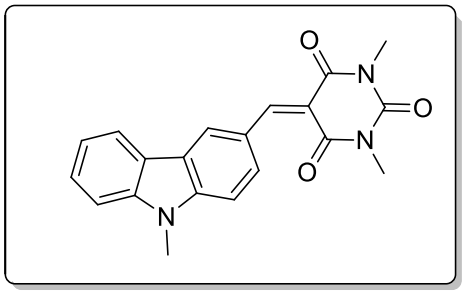

1,3-dimethyl-5-((9-methyl-9H-carbazol-3-yl)methylene)pyrimidine-2,4,6(1H,3H,5H)-trione (D2): Yellow solid; mp 246-248°C; 95% yield; IR (MIR-ATR, 4000-600cm^{-1}):ν_{max}= 1663, 1542, 1466, 1411, 1360, 1249, 1151, 1089, 787, 745, 607, 567 cm^{-1}; ^{1}H NMR (400 MHz, $CDCl_3$) δ ppm= 3.44(d, *J* = 1, 6H), 3.9(s, 3H), 7.37-7.33(m,1H), 7.44(dd, *J* = 8.3 and 5.9, 2H),7.55-7.52(m, 1H), 8.19(d, *J* = 7.8, 1H), 8.52(dd, *J* = 8.8 and 1.5, 1H), 8.77(s, 1H), 9.26(d, *J* = 1.5, 1H); ^{13}C NMR (100 MHz, $CDCl_3$) δ ppm = 28.42, 29.07, 29.44, 108.31, 109.19, 112.84, 120.79, 120.88 ,123.12, 123.96, 126.81, 129.91, 134.41, 141.66, 144.38, 151.61, 160.52, 161.23, 163.52; HR-MS (ESI$^+$) *m/z* calculated for $C_{20}H_{17}N_3O_3Na^+$ [M + Na^+]: 370.12; found: 370.1158.

(4) General Procedure for preparation of (E) and (Z)-3-((9-methyl-9H-carbazol-3 yl)methylene)indolin-2-one(7): [20a]

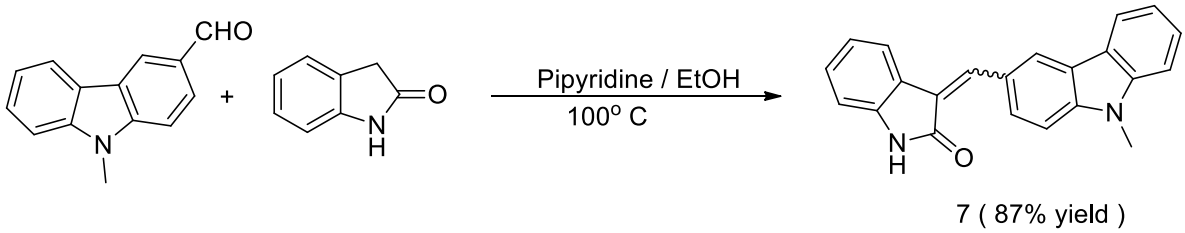

7 (87% yield)

To a solution of indolin-2-one (1 equiv.) in ethanol was added piperidine (0.30 mL) and 9-methyl-9H-carbazole-3-carbaldehyde (6) (1.2 equiv.) below 20° C. After complete addition, the reaction was stirred under reflux for 6 h. The reaction mixture was poured into 50 mL of ice water and the precipitate collected and washed with water. The mixture (3:1) of (E) and (Z)-3-((9-methyl-9H-carbazol-3 yl)methylene)indolin-2-one is then dried over vacua to get excellent yield.

(5) General Procedure for preparation of (E) and (Z)-1-acetyl-3-((9-methyl-9H-carbazol-3-yl)methylene)indolin-2-one (D3):

To a solution of 3-((9-methyl-9H-carbazol-3 yl)methylene)indolin-2-one (1.5 mmoles) in DMF (10 mL) was added NaH (60% dispersion in mineral oil, 1.5 mmoles). The yellow solution was stirred at room temperature for 15 minutes and turned red. Then acetic anhydride (3 mmoles) was added to the reaction mixture dropwise. The solution turned back to yellow and a precipitate formed. After 2 hours the solid was filtrated, washed with water and dried in vacua to afford a title compound as an orange-yellow solid (mixture of E and Z in 3:1 ratio).

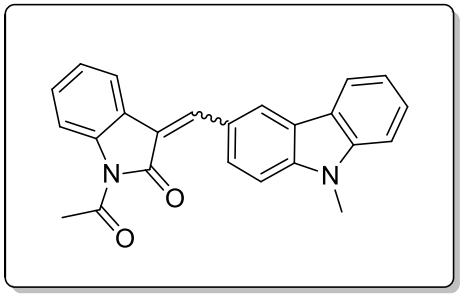

1-acetyl-3-((9-methyl-9H-carbazol-3-yl)methylene)indolin-2-one (D3): Orange-yellow solid; mp 160-162°C; 95% yield; IR (MIR-ATR, 4000-600cm^{-1}):ν_{max}= 2983, 2516, 2383, 2147, 2013, 1954, 1694, 1581, 1468, 1330, 1145, 1099, 744, 669, 579, 532 cm^{-1}; ^{1}H NMR (400 MHz, $CDCl_3$, mixture of the E and Z isomers, signals of the predominant isomer is given) δ ppm= 2.77(s, 3H), 3.86(s, 3H), 7.05-7.01(m, 1H), 7.32-7.2(m, 3H), 7.43-7.37(m, 2H), 7.54-7.49(m, 1H), 7.81(dd, *J* = 8.8 and 1.5, 1H), 7.97(d, *J* = 7.3, 1H), 8.08-8.06(m, 1H), 8.34(d, *J* = 7.8, 1H), 8.48-8.42(m, 1H); ^{13}C NMR (100 MHz, $CDCl_3$) δ ppm = 27.09, 29.33, 108.22, 108.66, 108.99, 116.68, 119.99, 120.52, 121.19, 122.55, 122.63, 123.03, 123.14, 124.35, 124.90, 126.62, 127.84, 129.54, 130.95, 139.8, 140.94, 141.54, 142.04; HR-MS (ESI$^+$) *m/z* calculated for $C_{24}H_{18}N_2O_2Na^+$ [M + Na^+]: 389.13; found: 389.1255.

4. References

1. Lewis, N. S. *Science*, **2007**, *315*, 798.

2. (a) Grätzel, M. *Chem. Lett.* **2005**, *34*, 8. (b) U.S Energy information Administration, 2008

3. O'Regan, B.; Grätzel, M. *Nature*, **1991**, *353*, 737.

4. P. R. F. Barnes, A. Y. Anderson, S. E. Koops, J. R. Durrant, and B. C. O'Regan, *Journal of Physical Chemistry C* **2009**, *113*, 1126.

5. U. Wurfel, M. Peters, and A. Hinsch, *Journal of Physical Chemistry C* **2008**, *112*, 1711. (b) L. Peter. *Accounts of Chemical Research* **2009**, *42*, 1839.

6. M. Murayama and T. Mori, *Journal of Physical Chemistry C* **2008**, *516*, 2716.

7. (a) O'Regan, B.; Grätzel, M. *Nature*, **1991**, *353*, 737. (b) Nature Chemistry, **2014**, *6*, 242.

8. M. Grätzel, *Research and Applications*, **2006**, *14*, 429.

9. J. Barber and B. Andersson, *Nature*, **1994**, *370*, 31.

10. G. Rothenberger, D. Fitzmaurice and M. Grätzel, J. *Phys. Chem*, **1992**, *96*, 5983.

11. C. J. Barbé, F. Arendse, P. Comte, M. Jirousek, F. Lenzmann, V. Shklover and M. Grätzel, *Journal of the American Ceramic Society*, **1997**, *80*, 3157.

12. Matthews, D., et al., *Solar Energy Materials & Solar Cells*, **1996**, *44*, 119.

13. (a) S. Ito, H. Miura, S. Uchida, M. Takata, K. Sumioka, P. Liska, P. Comte, P. Pechy, M. Grcatzel, *Chem. Commun*. **2008**, 5194. (b) W. Zeng, Y. Cao, Y. Bai, Y. Wang, Y. Shi, M. Zhang, F. Wang, Y. Pan, P. Wang, *Chem. Mater*., **2010**, *22*, 1915.

14. (a)Seo KD, Song HM, Lee MJ, Pastore M, Anselmi C, Angelis FD, *Dyes and Pigments.*,**2011**, *90*, 304. (b)T. Ono, T. Yamaguchi, H. Arakawa, *Solar Energy Materials & Solar Cells.,* **2009**, *93*, 831. (c)M. Matsui, M. Kotani, Y. Kubota, K. Funabiki, JY. Jin, T. Yoshida, *Dyes and Pigments* **2011**, *91*, 145. (d)M. Matsui, T. Fujita, Y. Kubota, K. Funabiki, JY. Jin, T. Yoshida, *Dyes and Pigments* **2010**, *86*, 143. (e)K. Hara, T. Sato, R. Katoh, A. Furube, T. Yoshihara, Murai.,*Advanced Functional Materials*,**2005**, *15*, 246. (f)Y. S. Chen, C. Li , Z. H. Zeng, W. B. Wang, X. S. Wang, B. W. Zhang., *Journal of Materials Chemistry.*,**2005**, *15*, 1654. (g) Im H, Kim S, Park C, Jang SH, Kim CJ, Kim K, *Chemical Commun*., **2010**,1335. (h) Kim D, Lee JK, Kang SO, J. Ko, *Tetrahedron.*, **2007**, *63*, 1913. (i) C. Zafer, B. Gultekin, C. Ozsoy, C. Tozlu, B. Aydin, S. Icli. *Solar Energy Materials & Solar Cells.*,**2010**, *94*, 655. (J) Z. Q. Wan, C. Y. Jia, Y. D. Duan, J. Q. Zhang, Y. Lin, Y. Shi., *Dyes and Pigments* **2012**, *94*, 150.

14b. *Int. J. Mol. Sci.* **2010**, *11*, 329.

15. (a)W. J. Wu, J. B. Yang, J. L. Hua, J. Tang, L. Zhang, Y. T. Long., *Journal of Materials Chemistry.*,**2010**, *20*, 1772. (b) M. H. Tsao, T. Y.Wu, H. P. Wang, I. W. Sun, S. G. Su,Y.C. Lin, *Materials Letters.*, **2011**, *65*, 583. (c) T. P. Brewster, S. J. Konezny, S. W. Sheehan, L. A. Martini, C. A. Schmuttenmaer, V. S. Batista, and R. H. Crabtree *Inorg. Chem*., **2013**, *52*, 6752.

16. Amaresh Mishra, Markus K. R. Fischer, and Peter Bauerle: *Angew. Chem. Int. Ed*. **2009**, *48*, 2474.

17. Kim D, Lee JK, Kang SO, J. Ko, *Tetrahedron.*, **2007**, *63*, 1913.

18. Staub, K.; Levina, G.A.; Fortd, A. *J. Mater. Chem.* **2003**, *13*, 825.

19. (a) José M. Fraile, Karel Le Jeune, José A. Mayoral, Nicoletta Ravasio Federica Zaccheria *Org. Biomol. Chem.*, **2013**, *11*, 4327. (b) B. Bandgar et al. *Journal of Enzyme Inhibition and Medicinal Chemistry*, **2013**, *28*, 593.

20. (a) G. M. O. Amombo et al. *Bioorg. Med. Chem. Lett.* **2012**, *22*, 7634. (b) R. R. Yadav et al. *Tetrahedron Letters* **2012**, *53*, 2222.

21. Becke, A.D. *J. Chem. Phys.* **1993**, *98*, 5648.

22. Becke, A.D. *J. Chem. Phys.* **1992**, *96*, 2155.

23. Lee, C.; Yang, W.; Parr, R.G. *Phys. Rev. B* **1988**, *37*, 785.

24. H.S. Nalwa, Handbook of advanced electronic and photonic materials and devices; Academic: San Diego, **2001**.

25. P. Naresh Kumar, Remya Narayanan, Melepurath Deepa, Avanish Kumar Srivastava *J. Mater. Chem. A*, **2014**, *2*, 9771.

5. Spectra

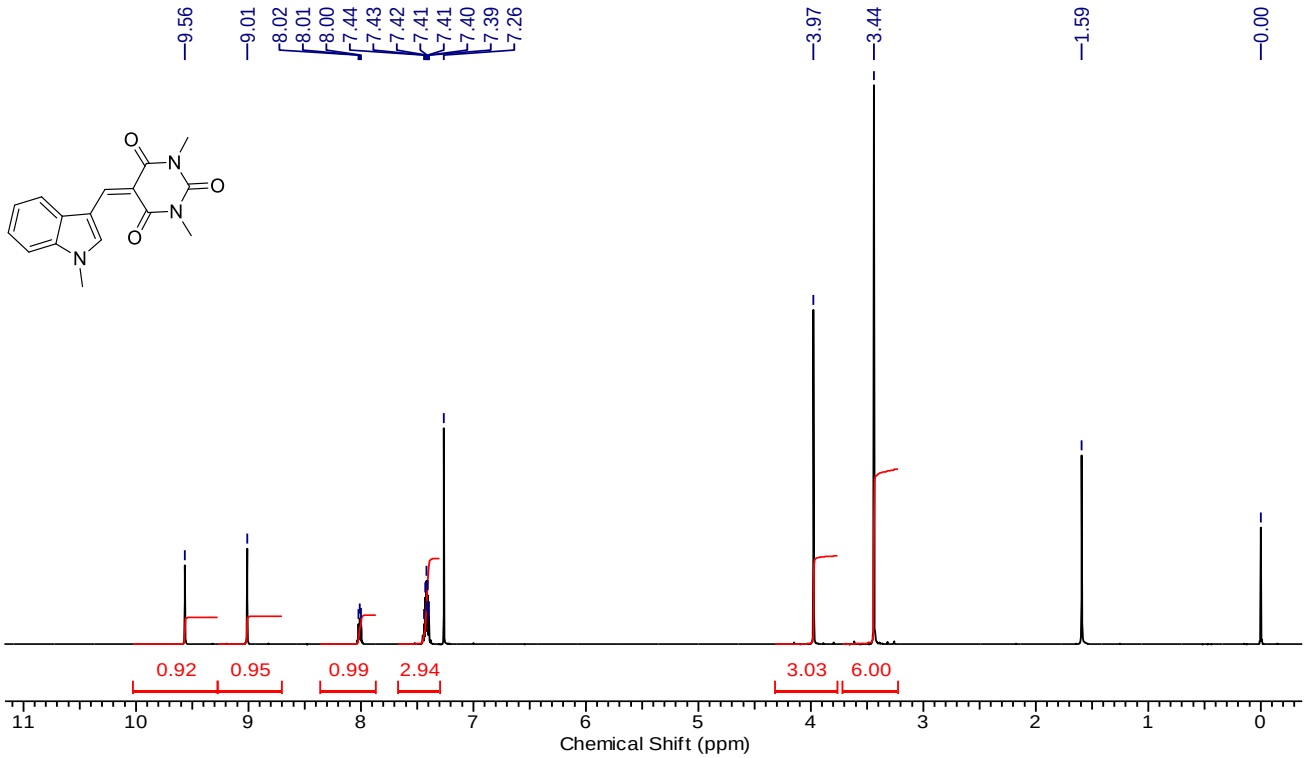

Figure 5.1.^{1}H NMR (400MHz) spectrum of compound **D1** in $CDCl_3$

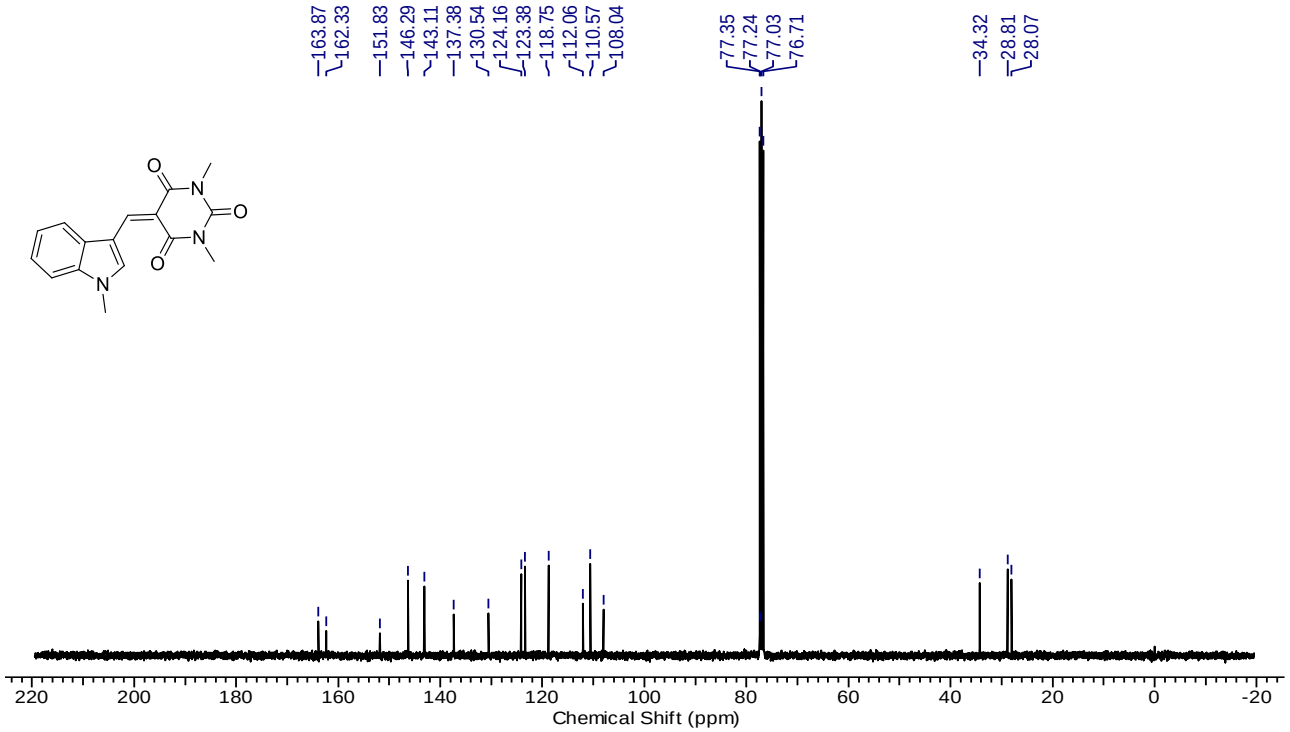

Figure 5.2.^{13}C NMR (400 MHz) spectrum of compound **D1** in $CDCl_3$.

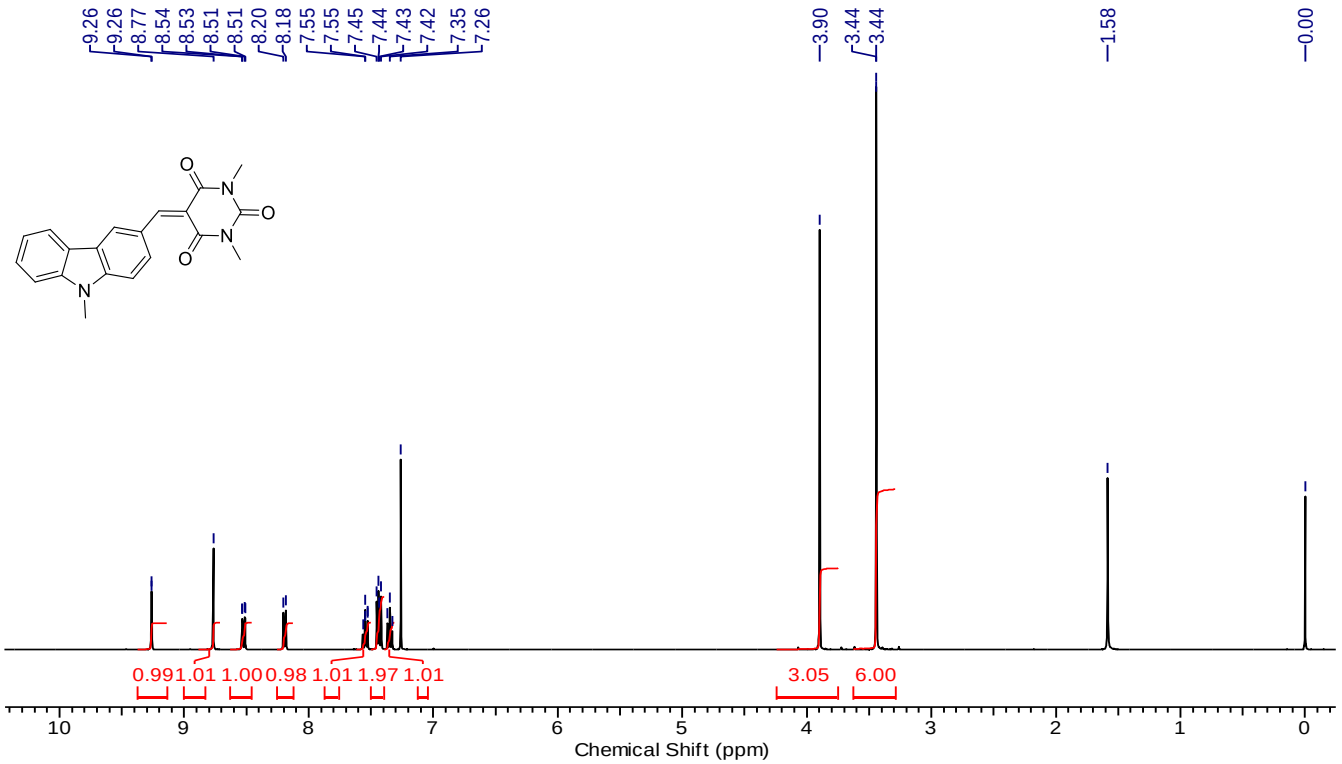

Figure 5.3. ^{1}H NMR (400MHz) spectrum of compound **D2** in $CDCl_3$

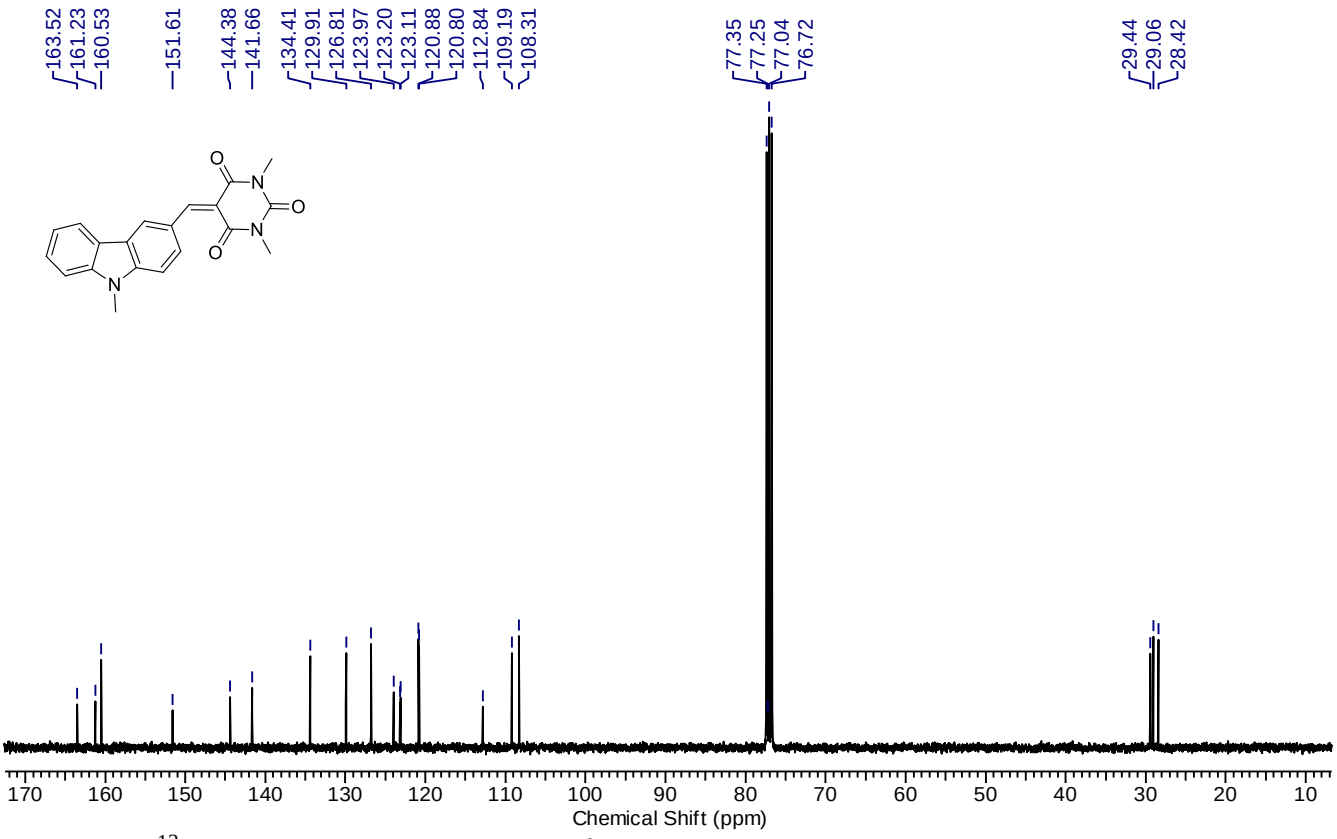

Figure 5.4. ^{13}C NMR (400 MHz) spectrum of compound **D2** in $CDCl_3$

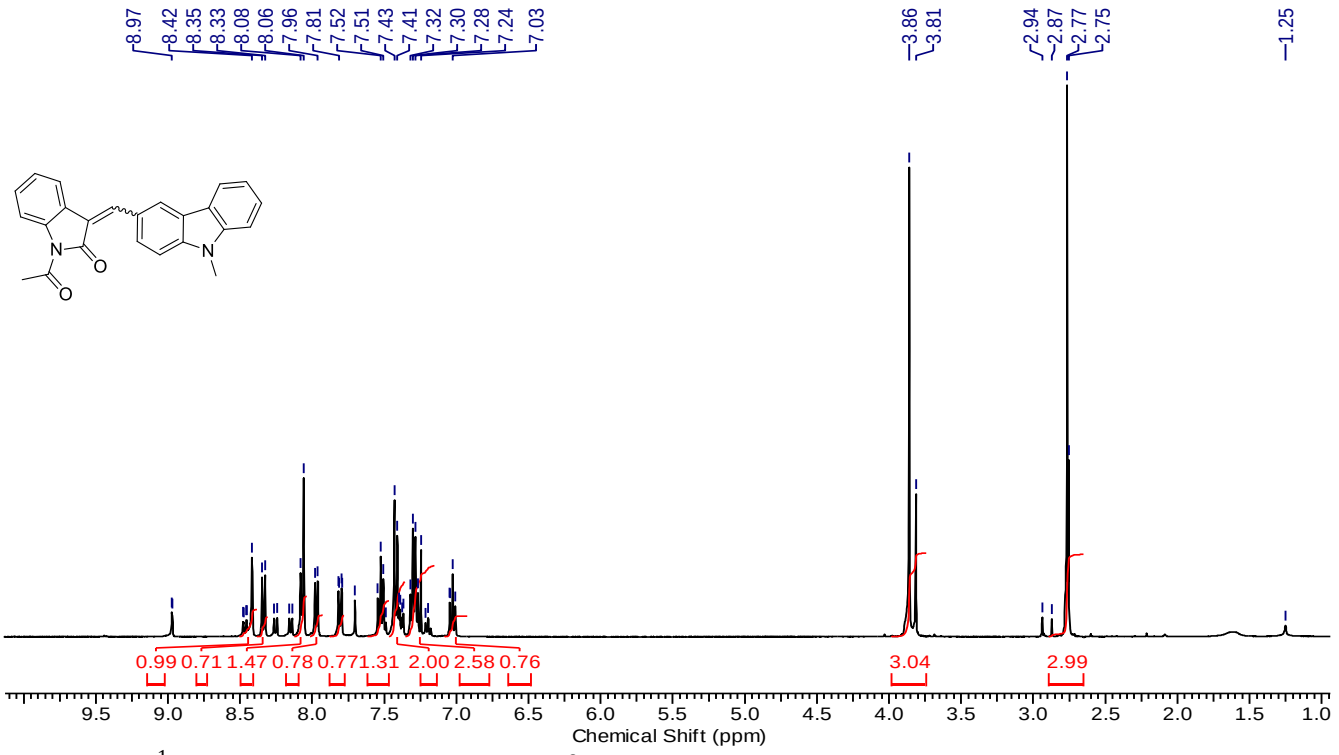

Figure 5.5. ^{1}H NMR (400MHz) spectrum of compound **D3** in $CDCl_3$

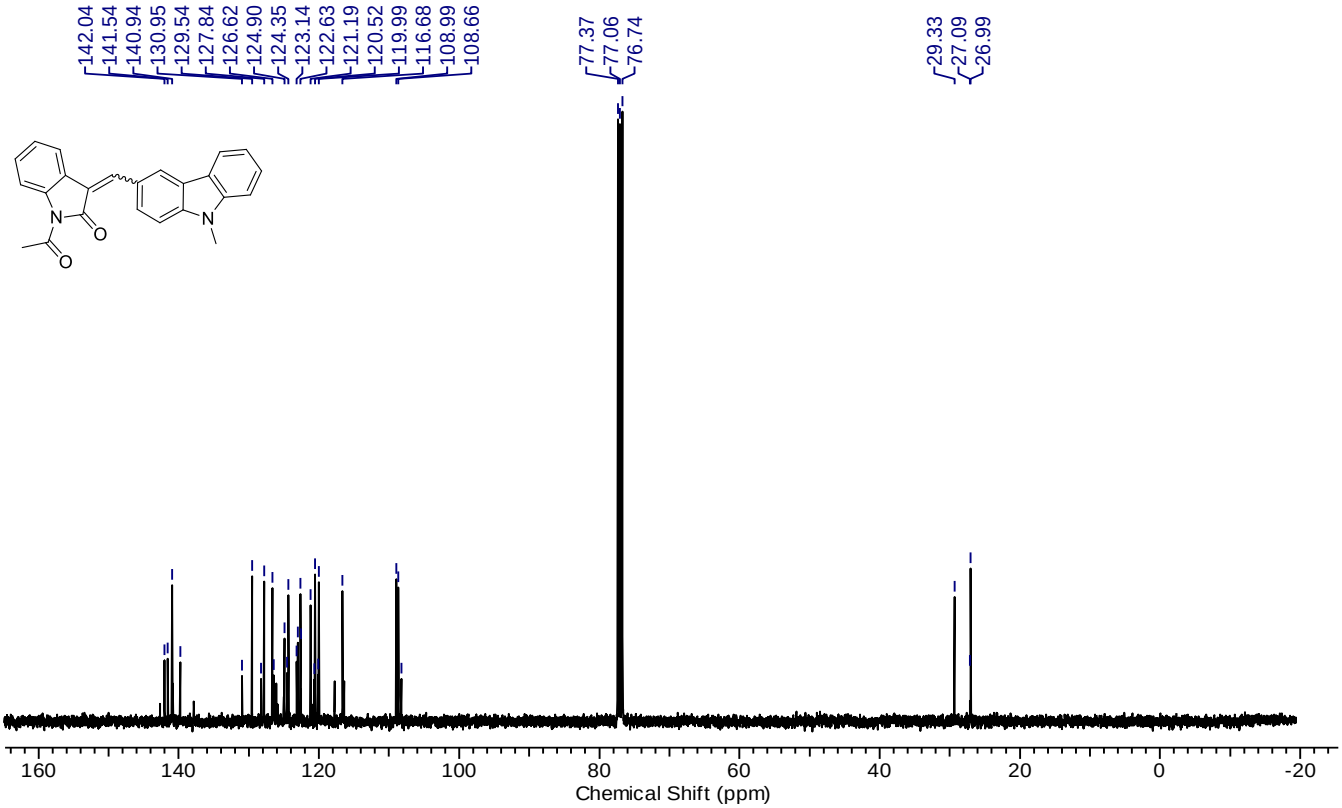

Figure 5.6. ^{13}C NMR (400 MHz) spectrum of compound **D3** in $CDCl_3$